

Review

Homogeneous Metal-Catalyzed Hydrogenation of CO₂ Derivatives: Towards Indirect Conversion of CO₂ to Methanol

Tolganay Andizhanova ¹, Aziza Adilkhanova ^{2,†} and Andrey Y. Khalimon ^{1,3,*} 

¹ Department of Chemistry, School of Sciences and Humanities, Nazarbayev University, 53 Kabanbay Batyr Avenue, Astana 010000, Kazakhstan; tolganay.andizhanova@nu.edu.kz

² School of Mining and Geosciences, Nazarbayev University, 53 Kabanbay Batyr Avenue, Astana 010000, Kazakhstan; aziza.adilkhanova@nu.edu.kz

³ The Environment and Resource Efficiency Cluster (EREC), Nazarbayev University, 53 Kabanbay Batyr Avenue, Astana 010000, Kazakhstan

* Correspondence: andrey.khalimon@nu.edu.kz; Tel.: +7-717-270-9102

† Current address: Department of Chemistry, Brock University, 1812 Sir Isaac Brock Way, St. Catharines, ON L2S 3A1, Canada.

Abstract: The increase in anthropogenic CO₂ concentrations and associated environmental issues have demanded the development of technologies for CO₂ utilization. Among various potential solutions to decrease CO₂ emissions and achieve carbon neutrality, the recycling of post-combustion CO₂ into value-added chemicals and fuels is considered one of the most economically attractive processes. In this regard, due to its large global demand and versatile applications in the chemical and energy sectors, methanol serves as the most appealing target for the chemical utilization of CO₂. However, direct hydrogenation of CO₂ to MeOH has proved challenging due to selectivity issues and high energy input, mainly dependent on CO₂-emitting fossil energy sources. To address these challenges, an alternative indirect CO₂-to-MeOH methodology has been proposed, which involves the hydrogenation of CO₂ via the intermediate formation of well-known CO₂ derivatives, such as formates, carbonates, formamides, carbamates, and urea derivatives. Homogeneous transition metal catalysts have been at the center of this research avenue, potentially allowing for more selective and low-temperature alternative routes from CO₂ to MeOH. This review aims to highlight the advances and challenges in homogeneous transition metal-catalyzed hydrogenation of major CO₂ derivatives to MeOH. Special attention is paid to the mechanisms of such transformations.

Keywords: homogeneous catalysis; carbon dioxide; hydrogenation; formates; carbonates; formamides; carbamates; urea derivatives



Citation: Andizhanova, T.; Adilkhanova, A.; Khalimon, A.Y. Homogeneous Metal-Catalyzed Hydrogenation of CO₂ Derivatives: Towards Indirect Conversion of CO₂ to Methanol. *Inorganics* **2023**, *11*, 302. <https://doi.org/10.3390/inorganics11070302>

Academic Editors: Maurizio Peruzzini and Francis Verpoort

Received: 22 June 2023
Revised: 14 July 2023
Accepted: 14 July 2023
Published: 15 July 2023



Copyright: © 2023 by the authors. Licensee MDPI, Basel, Switzerland. This article is an open access article distributed under the terms and conditions of the Creative Commons Attribution (CC BY) license (<https://creativecommons.org/licenses/by/4.0/>).

1. Introduction

The development of technologies for the utilization of carbon dioxide is of paramount importance for industrial decarbonization and moving forward toward a low-carbon economy [1]. These measures are driven by global climate change, which due to the greenhouse effect has recently become an issue recognized by society. CO₂ is considered the primary greenhouse gas, and a steady increase in its atmospheric concentration has been observed in recent decades, reaching a total of 424 ppm in 2023 [2]. Even within the last decade, despite the 2015 Paris Agreement to reduce CO₂ emissions, signed by 196 countries/parties [3], atmospheric concentrations of CO₂ raised by 28 ppm from 396 ppm in 2013, which contributes to about 6.6% of the total current atmospheric CO₂ concentration [2].

There are two major approaches to achieve carbon neutrality when shifting towards a low-carbon economy, both based on balancing carbon emissions with carbon usage: CSS (Carbon Storage and Sequestration) and CCUS (Carbon Capture, Utilization and Storage) technologies [4–7]. With regards to CO₂ utilization, “physical” utilization, e.g.,

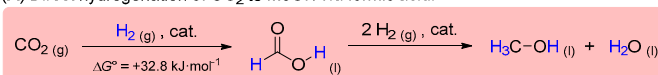
CO₂ as industrial fluid [8,9], the use of CO₂ for Enhanced Oil Recovery (EOR) [9,10], CO₂ storage in geological formations [11]) and chemical conversion of CO₂ to various value-added products are considered [5–7]. The latter option is more industrially attractive since CO₂ can serve as a relatively non-toxic and inexpensive C1 source and can be potentially converted into valuable chemical feedstock, fuel substitutes, polymers, and other useful materials [12,13]. In this regard, catalytic hydrogenation of CO₂ has been considered an attractive approach for CO₂ utilization, affording either C1-products (CO, CH₄, MeOH, Me₂O) or products of further derivatization, such as higher hydrocarbons, higher alcohols, etc. [14–18]. Among C1 products, methanol is the most appealing target [14] with a current annual global demand of 85 million tons, most of which is used to produce value-added chemicals [19]. Moreover, the future global methanol market is expected to grow at a rate of 4.24%, reaching about 136 million tons in 2032 [19]. Based on the growing market demand for methanol and given the fact that the cost of raw material feedstock strongly influences the overall product manufacturing expenses, the conversion of abundant and inexpensive CO₂ to methanol using “green” hydrogen could potentially lead to substantial economic and environmental benefits. Moreover, methanol is considered an appealing liquid hydrogen storage material that contains 12.6 wt.% of H₂ [20] and can be dehydrogenated on demand [21] or used directly in hydrogen transfer processes in the chemical industry [22].

Direct hydrogenation of CO₂ to MeOH is challenging due to the high stability of CO₂ ($\Delta G^\circ_{298} = -394.36 \text{ kJ}\cdot\text{mol}^{-1}$) and the thermodynamically unfavorable formation of formic acid (FA) (by $\Delta G^\circ = +32.8 \text{ kJ}\cdot\text{mol}^{-1}$) as an intermediate product (Scheme 1A) [23]. To overcome high activation barriers, early attempts in catalytic conversion of CO₂ to MeOH implied high reaction temperatures and pressures and/or aqueous media, which often resulted in undesired side reactions, such as overreduction of CO₂ to CH₄ and/or formation of CO, poisoning the catalysts [24]. To address these challenges, an alternative strategy for the reduction of CO₂ has been proposed, which involves indirect hydrogenation of CO₂ via the intermediate formation of the well-known CO₂ derivatives, such as formates, carbonates, formamides, carbamates, and urea derivatives (Scheme 1B) [16,24,25]. Such a tandem approach was suggested to lower the activation barriers, enabling conversion of CO₂ to MeOH under milder conditions, thus resulting in reduced amounts of unwanted side products (e.g., CO), which in turn diminishes the catalyst poisoning issues [24,25]. Moreover, many of the above CO₂ derivatives are currently produced on a large scale in industry [18,26]. For example, organic carbonates have great industrial potential as sustainable solvents and reagents [27,28], and their production from readily available diols and epoxides is considered one of the attractive venues for CO₂ utilization in industrial chemistry [29]. If epoxides are used as a feedstock, their reaction with CO₂ yields cyclic carbonates, the reduction of which results in a two-step strategy to convert CO₂ to methanol along with value-added diols derived from epoxides [24]. An analogous two-step route to MeOH from CO₂ can be anticipated via intermediate production of urea (about 180 million metric tons produced in 2022 with an estimated annual growth rate of about 4% until 2032 [30]) and urea derivatives [24].

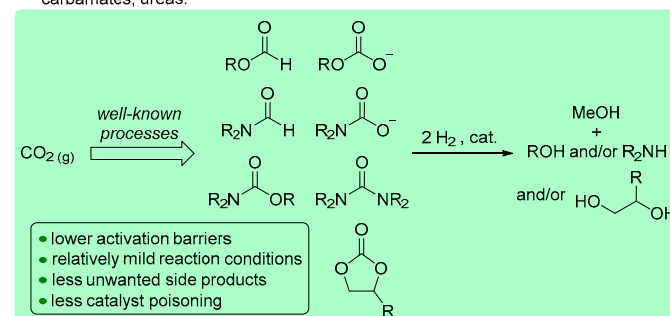
Considering the well-known routes to industrially relevant CO₂ derivatives [18,26,29], the development of an applicable indirect CO₂-to-MeOH methodology would require efficient and selective catalytic systems for the hydrogenation of these CO₂-derived products. Indeed, several transition metal complexes have been recently reported to catalyze these transformations, suggesting the potential viability of the two-step CO₂ reduction strategy depicted in Scheme 1B. The reactivity of CO₂ derivatives in catalytic hydrogenation reactions strongly depends on the electrophilicity of the carbonyl group and follows the trend of formates > formamides > carbonates > carbamates > ureas [24]. Early examples of hydrogenation of these compounds employed catalytic systems based on precious metal complexes (mostly Ru) [24,25]. However, due to low natural abundance and the recognized toxicity of these metals, the development of more economical and environmentally benign 3d metal surrogates became an important research venue. This comprehensive review aims to highlight the advances and challenges in the catalytic hydrogenation of major

classes of organic CO₂ derivatives and to demonstrate applications of these systems in the tandem conversion of CO₂ to MeOH. The present work is focused on homogeneous catalysts for the conversion of formates, formamides, carbonates, carbamates, and ureas to methanol. The discussion will be structured based on the classes of CO₂ derivatives and will include catalytic systems from the first examples through to the most recent advancements as of the beginning of 2023. Special attention will be paid to the mechanisms of catalytic hydrogenation reactions. Several reviews on homogeneous hydrogenation of CO₂ to methanol, including some examples of tandem approaches, have been recently published [24,25]; however, these accounts are mainly focused on transformations starting from CO₂, and rather limited examples of hydrogenation of substrates potentially derived from CO₂ have been discussed. Recent achievements in the related transfer hydrogenation of CO₂ derivatives have been comprehensively reviewed elsewhere [31]. The following parts of the manuscript will discuss the developments of hydrogenation catalysts based on the relative reactivity of CO₂ derivatives (from the most reactive formates to the least reactive ureas) and on the identity of transition metal catalysts (from conventional precious metal systems to abundant base metal catalysts).

(A) Direct hydrogenation of CO₂ to MeOH via formic acid:



(B) Indirect hydrogenation of CO₂ to MeOH via formamides, carbonates, carbamates, ureas:



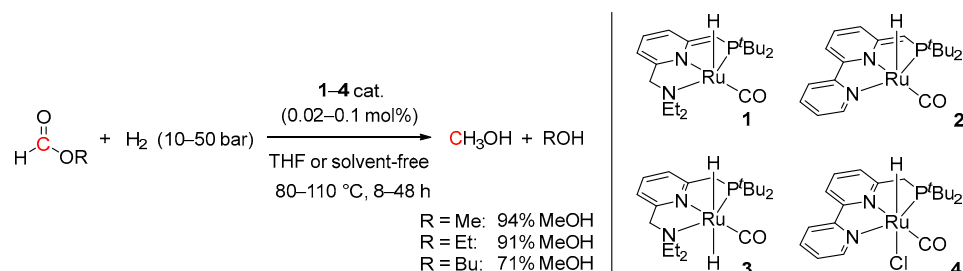
Scheme 1. Direct (A) and indirect (B) hydrogenation of CO₂ to methanol.

2. Catalytic Hydrogenation of Formates

Ammonium formates are considered as intermediate products in the hydrogenation of CO₂ to methanol in the presence of amines. Using this strategy, the initially formed ammonium formates are then condensed to formamides, which undergo further deaminative hydrogenation to MeOH. Such an approach using amines as CO₂ shuttle reagents is described in Section 3 of the manuscript (*vide infra*). In contrast, this section will concentrate on the hydrogenation of organic formates, such as methyl and ethyl formates, and the use of this strategy for the sequential reduction of CO₂ in the presence of alcohols. For example, methyl formate is considered as a readily available CO₂ derivative produced either by carbonylation of methanol [16] or by hydrogenation of CO₂ in the presence of MeOH [16,17].

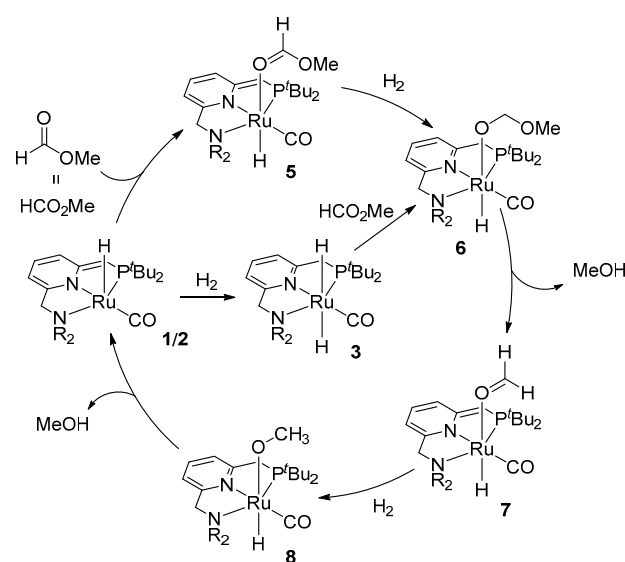
Although the synthesis of MeOH via methyl formate was first proposed in 1919, and several heterogeneous catalytic systems for hydrogenation of methyl formate to MeOH under high pressures and temperatures have been reported [32,33], probably the first example of a homogeneous catalytic system for hydrogenation of alkyl formates to MeOH was demonstrated by the Milstein group in 2011 [34]. The reactions were performed using a series of Ru-PNN complexes (1–4; Scheme 2) with the maximum turnover number (TON) for MeOH of 4700 (94% yield) observed for the bipyridine-derived catalyst 2 at only 0.02 mol% loading. In THF, 10–50 bar of H₂ were required and the optimal reaction temperature was found to be 110 °C. Analogously, 2-catalyzed hydrogenation of ethyl formate and n-butyl formate resulted in 91% and 71% of MeOH, respectively. Notably, at

0.1 mol% loading of **2**, methyl formate could be hydrogenated to MeOH with 98% yield (TON = 980) under solvent-free conditions and low temperature (80 °C) and H₂ pressure (10 bar), demonstrating a “greener” approach to MeOH production.



Scheme 2. Ru PNN-catalyzed hydrogenation of alkyl formates to MeOH.

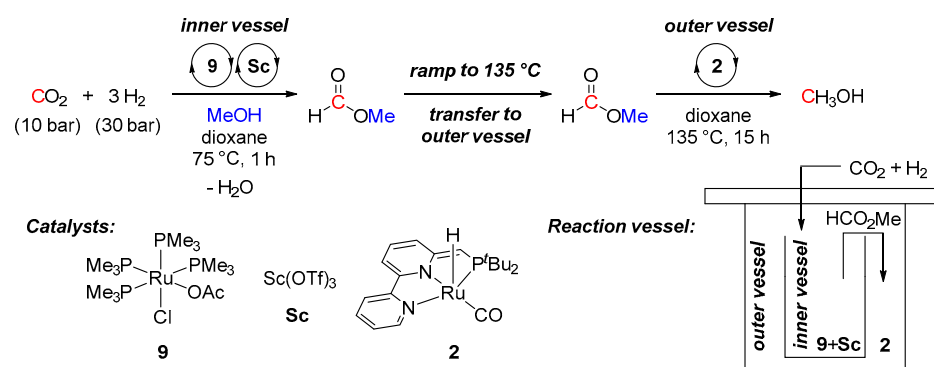
Considering the well-known ability of complex **1** to heterolytically split H₂ and produce the dihydride complex **3**, and based on the stoichiometric reactivity of **3** with methyl formate, which showed a stepwise formation of the Ru(II) formaldehyde and methoxy species (**7** and **8**, respectively; Scheme 3), a metal-ligand cooperative (MLC) mechanism for Ru-PNN-catalyzed hydrogenation reactions was suggested. Starting with the dearomatized species **1** or **2**, coordination of the methyl formate to Ru gives complex **5**. This is followed by the addition of H₂ and the hydride transfer to the formate ligand to generate an intermediate **6**. The subsequent deprotonation of the benzylic side-arm of the PNN ligand by the methoxy group leads to the release of MeOH and formation of the formaldehyde species **7**, which then undergoes hydrogenation to the methoxy complex **8**. Lastly, the liberation of MeOH from **8** via ligand dearomatization regenerates the catalyst (Scheme 3). This general mechanistic proposal was further supported by DFT calculations, disclosed by Wang et al. in 2012 [35].



Scheme 3. A plausible mechanism for Ru PNN-catalyzed hydrogenation of HCO₂Me to MeOH.

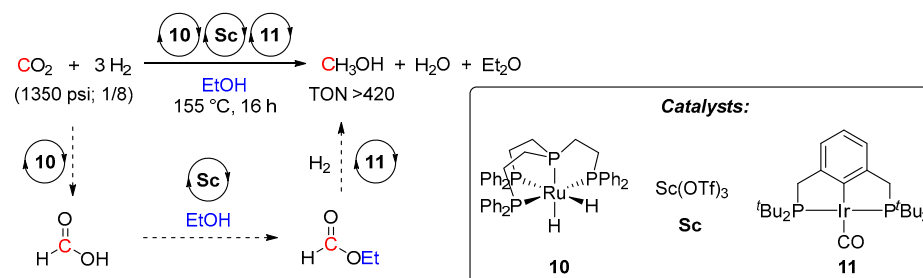
In 2011, Sanford et al. also applied complex **2** in a continuous cascade hydrogenation of CO₂ to MeOH with an intermediate formation of methyl formate [36]. Initially, a mixture of two different ruthenium catalysts (complexes **9** and **2** for CO₂-to-FA and formate-to-MeOH steps, respectively) and Sc(OTf)₃ (to accelerate the esterification of formic acid (FA) to methyl formate) was subjected to hydrogenation of CO₂ in CD₃OH (10 bar CO₂, 30 bar H₂, 135 °C, 16 h), showing only 2.5 turnovers for MeOH. As a result, despite an improved Lewis acid-promoted formation of methyl formate from CO₂, the addition of even 1 mol% of Sc(OTf)₃ significantly retards the following **2**-catalyzed hydrogenation of the formate to

MeOH. To overcome this issue, physical separation of the esterification and the formate-to-MeOH reaction sites was required (Scheme 4). Therefore, the reaction was repeated in a two-vessel (inner and outer) system. The first esterification step was performed at 75 °C in the inner vessel using a mixture of complex **9** and Sc(OTf)₃ as catalysts. The **2**-catalyzed hydrogenation of methyl formate to MeOH was performed in an outer vessel. For this, a temperature ramp to 135 °C was applied, which resulted in the transfer of the initially formed methyl formate (bp = 32 °C) from the inner to the outer vessel. This strategy allowed to prevent deactivation of catalyst **2** with Sc(OTf)₃ and provided 21 turnovers for MeOH. Further tuning of each of the individual catalytic steps and/or providing a better technological solution for the physical separation of esterification/hydrogenation steps could provide opportunities for the development of an applicable cascade catalytic approach to methanol from CO₂.



Scheme 4. Ru-catalyzed cascade catalytic reduction of CO₂ to MeOH.

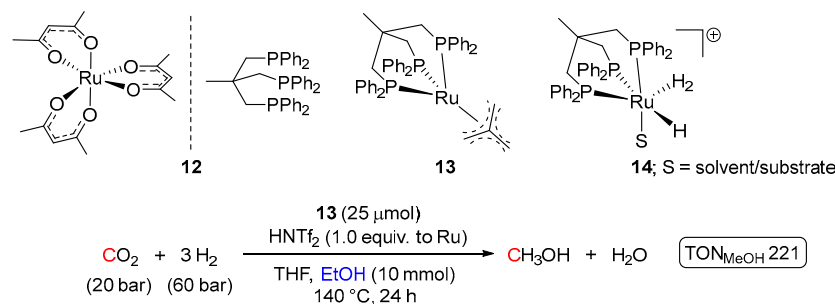
Analogous cascade hydrogenation of CO₂ to methanol was also reported by Goldberg et al. in 2019 [37]. Similarly, the overall process consisted of three steps: CO₂-to-FA hydrogenation, FA esterification to HCO₂Et, and hydrogenation of the formate intermediate to MeOH. The first two steps employed {P(CH₂CH₂PPh₂)₃}Ru(H)₂ (**10**) and Sc(OTf)₃ as catalysts, respectively, resembling Sanford's system. In the third formate-to-MeOH hydrogenation step, in contrast to Sanford's protocol, instead of an acid-sensitive Ru complex **2**, which showed rather a low turnover to MeOH, a more robust Ir(I) complex (PCP)Ir(CO) (**11**) was employed (Scheme 5). Such greater stability of **11** vs. **2** to Sc(OTf)₃ as well as the high thermal stability of **11** allowed tuning of the cascade CO₂ hydrogenation to afford > 420 turnovers to MeOH. However, gradual poisoning of catalysts **10** and **11** by CO, formed via decarbonylation of ethyl formate as a side-reaction, was postulated as a TON limiting factor.



Scheme 5. Ru/Ir-catalyzed cascade catalytic reduction of CO₂ to MeOH.

Considering applications of non-pincer Ru systems, Klankermayer and Leitner et al. disclosed one-pot hydrogenation of CO₂ to MeOH conducted in THF in the presence of EtOH and catalyzed by a Ru(II) complex bearing a Triphos ligand (Triphos = 1,1,1-tris(diphenyl-phosphinomethyl)ethane) (Scheme 6) [38]. Initially, the ruthenium pre-catalysts **12** and **13** were tested in the hydrogenation of both methyl and ethyl formates under 50 bar of H₂ at 140 °C, showing up to 77 TON to methanol in 24 h. The reactions

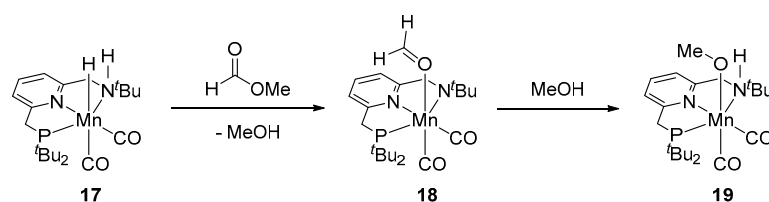
required acidic conditions to generate a cationic (Triphos)Ru species **14**, suggested as the active catalyst. Encouraged by these findings, and considering the well-known ability of Ru(II) phosphine complexes to hydrogenate CO₂ to formic acid (FA) and its derivatives [39,40], one-pot hydrogenation of CO₂ in the presence of EtOH and pre-catalysts **10** and **11** was attempted, showing after 24 h at 140 °C the maximum TON of 221 for **11**/HNTf₂ system (Scheme 6).



Scheme 6. (Triphos)Ru-catalyzed hydrogenation of CO₂ to MeOH in the presence of EtOH.

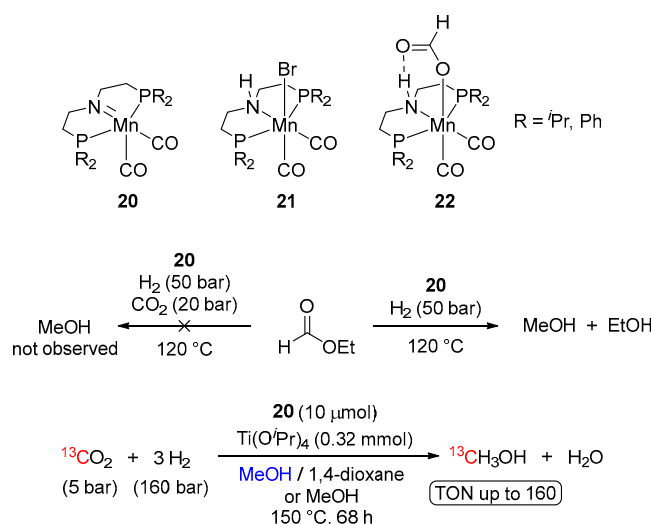
A similar approach for CO₂ hydrogenation to MeOH was also demonstrated by the Beller group in 2017, using a catalyst system based on Co(acac)₃/Triphos (**15**, acac = acetylacetonate) and HNTf₂ [41]. Conducting the reaction with 20 bar of CO₂ and 70 bar of H₂ in THF in the presence of EtOH for 24 h resulted in TON for MeOH of 50, which is lower compared to Ru-catalyzed reactions previously reported by Klankermayer and Leitner et al. [38]. However, the Co-catalyzed hydrogenation could be performed at lower temperatures (100 °C vs. 140 °C for Ru) without a decrease in the activity of the catalyst, representing a rare example of a non-noble metal system for the mild reduction of CO₂ to MeOH. Analogously to Ru, Co-catalyzed reactions were suggested to involve a cationic (Triphos)Co species, formed by a slow HNTf₂-assisted removal of acac ligands. However, in contrast to the analogous Ru system [38], the Co-catalyzed conversion of CO₂ to MeOH was proposed to take place through an inner-sphere mechanism that does not involve the intermediate formation of ethyl formate. Although small amounts of both FA and the formate were detected during the reaction, no significant accumulation of these products was seen during catalytic runs. Moreover, as the observed inconsistencies in the rates of hydrogenation of CO₂, FA and ethyl formate suggested that both FA and ethyl formate are only formed as by-products, being a part of a minor reaction pathway [41].

Another example of a base metal catalytic system for the hydrogenation of methyl formate to MeOH was reported by Milstein et al. in 2018 [42]. The reduction of HCO₂Me with an Mn(I) pincer complex (PNN^H)Mn(Br)(CO)₂ (**16**) was performed in toluene at 110 °C as a part of a stepwise process for hydrogenation of dimethyl carbonate (i.e., Me₂CO₃ → HCO₂Me → MeOH; vide infra) and resulted in 85% of MeOH in 30 h using 2 mol% loading of **16** (activated with 4 mol% of KH) and 30 bar of H₂. A hydride complex (PNN^H)Mn(H)(CO)₂ (**17**) was proposed as an active catalytic species, and to obtain some insights into the mechanism of this transformation the in situ generated complex **17** was treated with methyl formate to give a MeOH and a formaldehyde species (PNN)Mn(η¹-O=CH₂)(CO)₂ (**18**). Under catalytic hydrogenation conditions, **18** was proposed to convert to the methoxy complex (PNN^H)Mn(OMe)(CO)₂ (**19**), followed by the liberation of another equivalent of MeOH (Scheme 7). This reaction pathway largely resembles the MLC mechanism of hydrogenation of methyl formate to MeOH, previously proposed by the same group for analogous Ru-PNN complexes **1–4** (Scheme 3) [34,35], with the difference that the Mn system operates via an amine/amide cooperativity and does not involve dearomatization of the pyridine moiety of the PNN ligand.



Scheme 7. Reactivity of (PNN^H)Mn(H)(CO)₂ (**17**) with methyl formate.

The related reactivity of another bifunctional manganese pincer complex was recently disclosed by Leitner et al. [43]. The study was performed using an amide Mn(I) complex, (PNP)Mn(CO)₂ (**20**), which could be effectively generated by the treatment of the corresponding amine pre-catalyst (PN^HP)Mn(Br)(CO)₂ (**21**) with NaO^tBu. Although **20** was capable of hydrogenating ethyl formate to MeOH, no conversion of the formate to MeOH was observed in the presence of CO₂ (20 bar). This inhibiting effect of CO₂ was rationalized by the formation of a very stable Mn(I) formate intermediate **22** (Scheme 8), blocking the catalytic turnover. The catalytic activity of the system in the hydrogenation of CO₂ was unlocked by the addition of alcoholate Lewis acids (Ti(OⁱPr)₄ or Sc(OTf)₃), allowing removal of the formate ligand from **22**, freeing up of the coordination site at Mn, and efficient generation of the methyl formate intermediate. Thus, conducting **20**-catalyzed hydrogenation of CO₂ in the presence of Ti(OⁱPr)₄ in either a 1:1 (vol.) mixture of MeOH and 1,4-dioxane or pure MeOH and using 5 bar of ¹³CO₂ and 160 bar of H₂ resulted in 68 h at 150 °C in up to 160 TON for ¹³CH₃OH (Scheme 8). The proposed **20**-catalyzed reaction pathway resembles the mechanism for **2**-catalyzed transformation (Scheme 3) [34,35]. The detailed mechanistic studies supported by DFT calculations suggested an MLC outer-sphere route with turnover-determining transition states being associated with the concerted activation of H₂ by **20** and the Mn-assisted C-O bond cleavage of a hemiacetal intermediate, formed by hydrogenation of the formate [44].



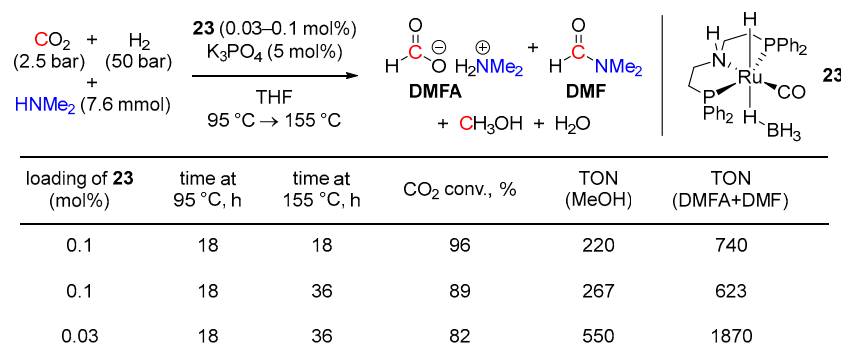
Scheme 8. Hydrogenation of ethyl formate and CO₂ catalyzed by Mn-PNP complexes.

3. Catalytic Hydrogenation of Formamides

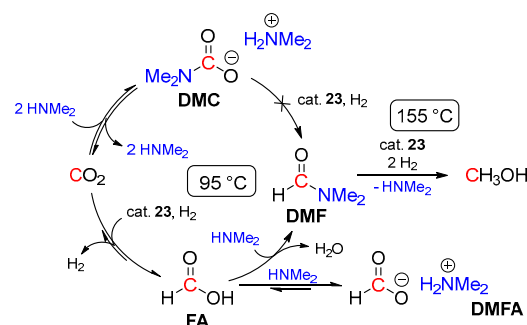
Together with ammonium formate salts, formamides are considered as intermediate products upon hydrogenation of CO₂ in the presence of amines [25]. Although, a number of transition metal complexes has been shown to reduce formamides to the corresponding methylamines via deoxygenation reactions (C-O bond cleavage) [45,46], catalytic systems for selective hydrogenation of formamides to methanol via C-N bond cleavage have been developed to a lesser extent [47].

Probably the first example of the homogeneous tandem hydrogenation of CO₂ to methanol with an intermediacy of dimethylformamide (DMF) was demonstrated by San-

ford and coworkers in 2015 using the ruthenium borohydride catalyst (PN^HP)Ru(H)(η^1 -BH₄)(CO) (**23**; Scheme 9) [48]. The reactions were conducted with 2.5 bar of CO₂ and 50 bar of H₂ in the presence of HNMe₂, 0.03–0.1 mol% of **23**, and 5 mol% of K₃PO₄ and resulted in 82–96% conversions of CO₂ to MeOH with turnover numbers up to 550 (Scheme 9). The proposed reaction mechanism is shown in Scheme 3 and involves a fast reversible formation of dimethylammonium dimethyl-carbamate (DMC) as a CO₂ capture step. Due to the very low electrophilicity of the carbonyl group in DMC, its direct hydrogenation to DMF was suggested to be problematic. Instead, the reversible release of CO₂ from DMC was proposed, followed by **23**-catalyzed hydrogenation of CO₂ to formic acid, driven by the amidation of the latter to DMF. In the last step, **23**-catalyzed hydrogenation of DMF furnishes MeOH. To achieve the proposed sequence, a single pot temperature ramp strategy was applied, where the reaction mixture was first heated at 95 °C for 18 h to ensure the initial equilibration of DMC and CO₂ and **23**-catalyzed hydrogenation of CO₂ to DMF. Subsequently, the temperature of the reaction was increased, and the next step, **23**-catalyzed hydrogenation of DMF to MeOH, was performed at 155 °C for 18–36 h (Scheme 10). Nonetheless, large quantities of the formate [HCO₂][H₂NMe₂] (DMFA) and DMF intermediates (up to 74% yield of the mixture) remained unreacted, which could be attributed to partial decomposition of the catalyst at high temperatures, and further improvements of the system were required to increase the conversion of CO₂ to methanol.



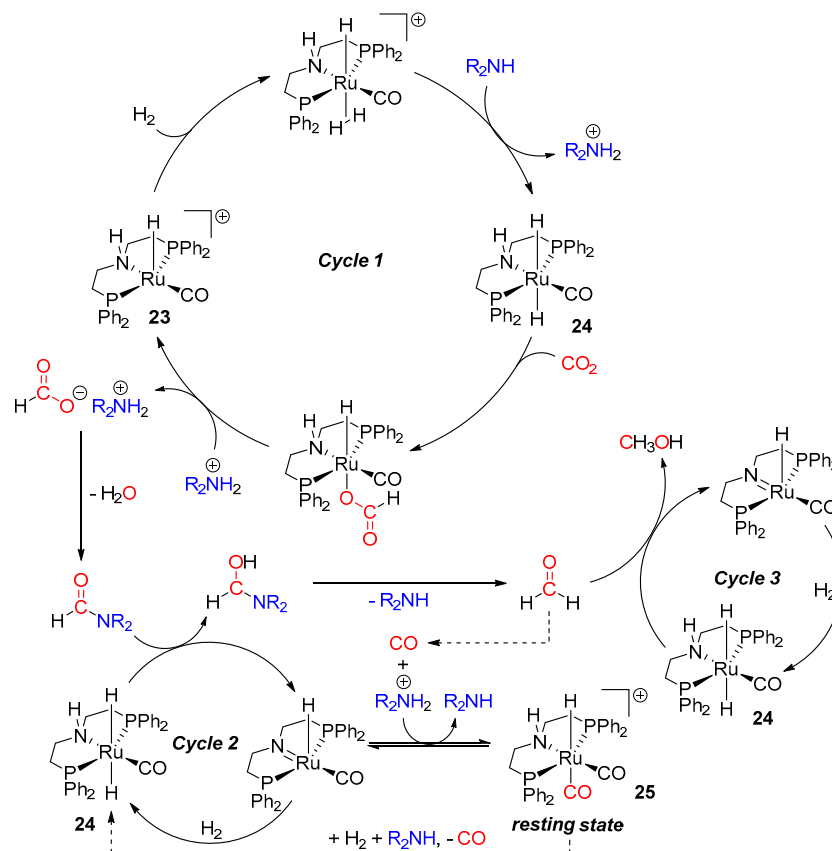
Scheme 9. **23**-catalyzed reduction of CO₂ to MeOH in the presence of HNMe₂.



Scheme 10. Proposed pathway for **23**-catalyzed hydrogenation of CO₂ to MeOH in the presence of HNMe₂.

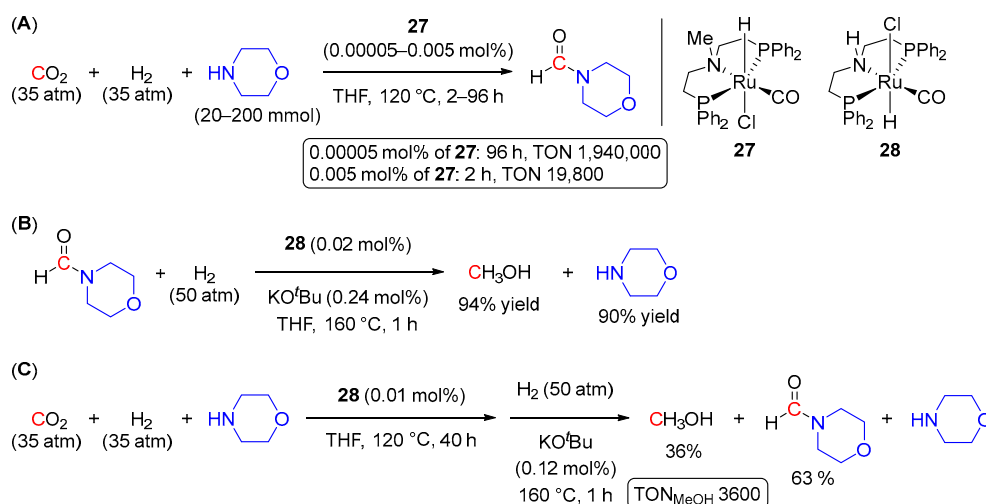
A plausible mechanism for **23**-catalyzed amine-assisted sequential hydrogenation of CO₂ to methanol was later proposed by Prakash et al. (Scheme 11) [49]. The reaction was suggested to start with the generation of the ruthenium mono-carbonyl dihydride species **24**, converting CO₂ to ammonium formate (cycle 1). This is followed by the condensation of the formate intermediate to the formamide product [50], which then undergoes **24**-catalyzed hydrogenation to hemiaminal (cycle 2). The latter derivative quickly decomposes to the starting amine and formaldehyde, which participates in the third **24**-catalyzed cycle to produce MeOH (cycle 3). Under high temperatures, formaldehyde could also decompose to CO, which in turn coordinates to Ru to give a dicarbonyl species [(PN^HP)Ru(H)(CO)₂]⁺

(25), observed experimentally and considered as the catalyst resting state. From here, the active Ru dihydride catalyst 24 can be rescued by the addition of H₂ and an amine to 25. Notably, based on control experiments with the closely related (PN^{Me}P)Ru(H)(Cl)(CO) (26), in which the N-H was replaced with N-Me, no ligand-assisted H₂ transfer to CO₂ in the first formate cycle (cycle 1, Scheme 11) was suggested. On the other hand, complex 26 was found to be inactive in the formamide and formaldehyde reduction steps, suggesting an MLC pathway (cycles 2/3, Scheme 11).



Scheme 11. The suggested mechanism for 23/amine-catalyzed hydrogenation of CO₂ to MeOH (BH₄[−] ligand in 23 is omitted for clarity).

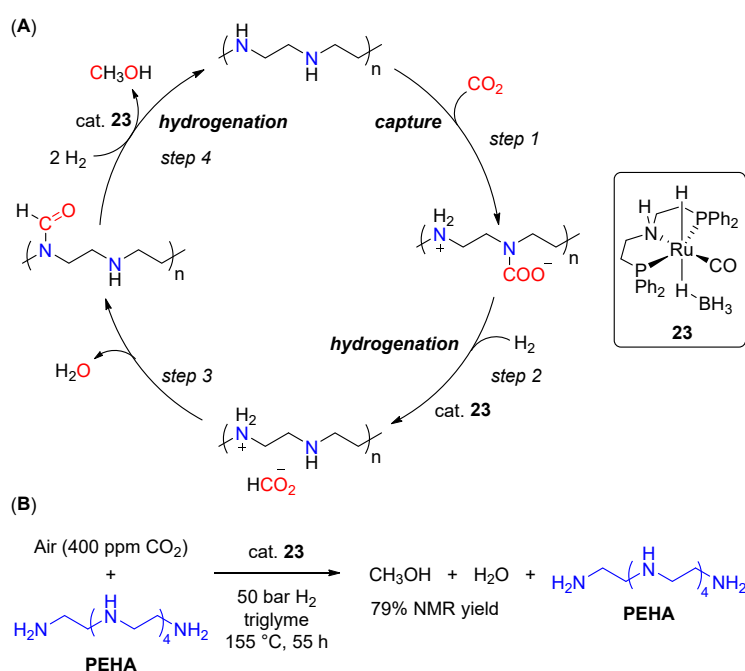
Almost at the same time as Sanford, Ding et al. disclosed a highly efficient *N*-formylation of a series of primary and secondary amines with H₂ and CO₂ to give the corresponding formamides using Ru pincer pre-catalysts 27 and 28, with the highest TON of 1,940,000 observed for morpholine (Scheme 12A) [51]. Notably, the catalyst was recycled up to 12 times without any significant loss of its activity, demonstrating its potential practical applicability. Using complex 28, the produced *N*-formyl-morpholine was also hydrogenated to MeOH with 94% yield (Scheme 12B). The sequential one-pot strategy for hydrogenation of CO₂ to MeOH in the presence of morpholine was also tested and resulted in 36% of MeOH with a TON of 3600 (Scheme 12C). Similarly to Sanford's approach [48], a temperature ramp strategy was applied, resulting in a two-step reaction, where the formation of *N*-formyl-morpholine was achieved at 120 °C (40 h), followed by the hydrogenation of *N*-formyl-morpholine to MeOH at 160 °C within 1 h. This temperature ramp was accompanied by the H₂ pressure increase from 35 atm in the first step to 50 atm in the second step. Despite moderate yields of MeOH (36%), the developed system shows significant improvement compared to the 23-catalyzed transformation reported by Sanford et al. (Scheme 9) [48] and opens further opportunities for integration of CO₂ capture and CO₂ functionalization approaches under one-pot conditions.



Scheme 12. (A) **27**-catalyzed *N*-formylation of morpholine; (B) **28**-catalyzed hydrogenation of *N*-formyl-morpholine to MeOH; (C) **28**-catalyzed one-pot two-step hydrogenation of CO₂ to methanol in the presence of morpholine.

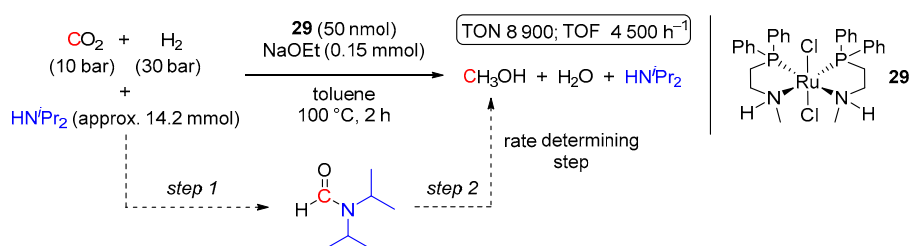
Inspired by these results, in 2016, Olah and Prakash et al. reported a more practical and robust CO₂ reduction catalytic system, capable of efficient capture of CO₂ from air [52]. Analogously, (PN^HP)Ru(H)(η¹-BH₄)(CO) (**23**) was used as a hydrogenation catalyst, but the capture of CO₂ was achieved using pentaethylene-hexamine (PEHA). Due to the high basicity of PEHA and its nonvolatile nature, efficient CO₂ trapping was achieved at high temperatures, and no temperature ramp for the hydrogenation of CO₂ to MeOH was required. The reaction was performed in THF directly at 155 °C using 75 bar CO₂/H₂ (1:3) in the presence of complex **23** (20 μmol) and PEHA (3.4 mmol), resulting at 200 h in 23% of MeOH (TON = 1060).

The overall reaction pathway for in situ hydrogenation is depicted in Scheme 13A and includes the PEHA-supported formation of the carbamate (step 1), formate (step 2), and formamide (step 3) intermediates. Notably, after hydrogenation of the formamide intermediate (step 4), the produced MeOH can be separated by a simple distillation, and the catalyst, solvent, and amine were reused up to five times, showing more than 75% of the initial activity after five cycles. Switching from THF to triglyme as the reaction medium, reducing the temperature to 145 °C and applying 75 bar pressure of a 1:9 mixture of CO₂/H₂, a cumulative TON of 2150 was obtained after five consecutive runs, suggesting potential applicability of the developed method in a flow-type continuous production of MeOH. Lastly, the developed CO₂-to-MeOH reduction system was tested in the hydrogenation of CO₂ captured from synthetic air (400 ppm of CO₂ in N₂/O₂ 80/20; Scheme 13B). After 55 h at 155 °C, a 79% yield of MeOH was observed, demonstrating the first example of a homogeneous system for the capture of CO₂ from the air and its direct conversion to methanol. Later on, the same catalyst was applied by Prakash et al. in PEHA-assisted CO₂-to-MeOH hydrogenation in a biphasic H₂O/2-methyltetrahydrofuran (2-MTHF) system, allowing for simple recycling of the catalyst and the amine without any significant loss in their effectiveness [53]. Interestingly, compared to PEHA, other polyamine auxiliaries as well as readily available mono-ethanolamine (MEA), showed significantly lower conversions of CO₂ to methanol, although comparable (or even greater compared to MEA) effectiveness of some of these amines in the CO₂ capture step was observed.



Scheme 13. (A) Proposed reaction pathway for CO₂ capture and in situ **23**-catalyzed hydrogenation of CO₂ to MeOH using a polyamine; (B) **23**/pentaethylene-hexamine-catalyzed capture of CO₂ from air and conversion to MeOH.

An impressive catalytic CO₂ hydrogenation activity of RuCl₂(Ph₂PCH₂CH₂NHMe₂)₂ (**29**) with HN^{*i*}Pr₂ auxiliary was demonstrated by Wass et al. in 2017 [54]. The reaction was performed in a one-pot manner under rather mild conditions (100 °C, 2 h, 10 bar CO₂, 30 bar H₂) and low catalyst loading of 50 nmol and showed the selective formation of MeOH, surpassing previously reported homogeneous catalysts in terms of TON (up to 8900) and TOF (up to 4500 h⁻¹) by at least an order of magnitude (Scheme 14).

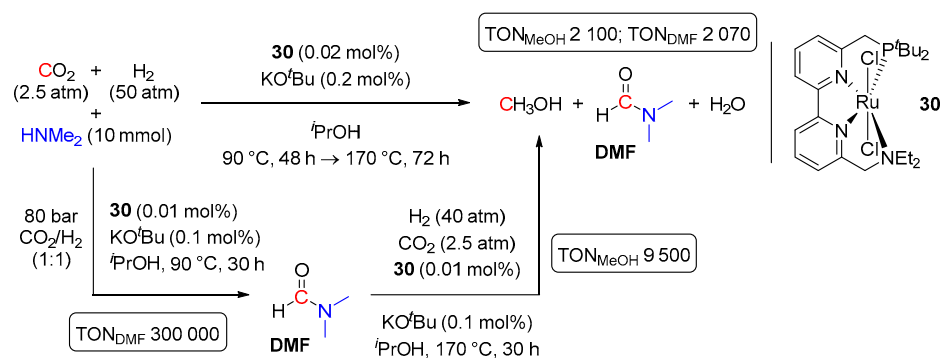


Scheme 14. **29**-catalyzed selective reduction of CO₂ to MeOH in the presence of HN^{*i*}Pr₂.

Notably, the nature of the amine auxiliary in **29**-catalyzed CO₂-to-MeOH hydrogenation had a strong influence on the outcome of the reaction. Gradually decreasing the steric hindrance of an amine from HN^{*i*}Pr₂ to HN^{*n*}Pr₂, HNEt₂, and finally to HNMe₂ resulted in decreased MeOH yields, and the formation of large quantities of the corresponding formamide intermediates was detected (from TON_{amide} of 0 for HN^{*i*}Pr₂ to 14,000 for HNMe₂). Such an improved performance of bulkier amines in the production of MeOH was rationalized by their reduced tendency to bind to the catalyst as well as by faster hydrogenation of bulkier amide intermediates (step 2 in Scheme 14; rate-determining step) [54].

Several other Ru-based catalysts for direct amine-assisted hydrogenation of CO₂ to methanol have been reported since 2017 [55,56], albeit that these systems demonstrated lower catalytic activities, compared to **29**-catalyzed transformation. Thus, in 2018, Zhou and co-workers disclosed a one-pot hydrogenation of CO₂ to MeOH in the presence of HNMe₂ and a ruthenium catalyst **30** bearing a tetradentate PNNN ligand (Scheme 15) [55]. The reactions proceeded via an intermediate formation of DMF and were conducted in isopropanol with 2.5 atm of CO₂ and 50 atm of H₂, 0.02 mol% of **30**, and 0.2 mol% of

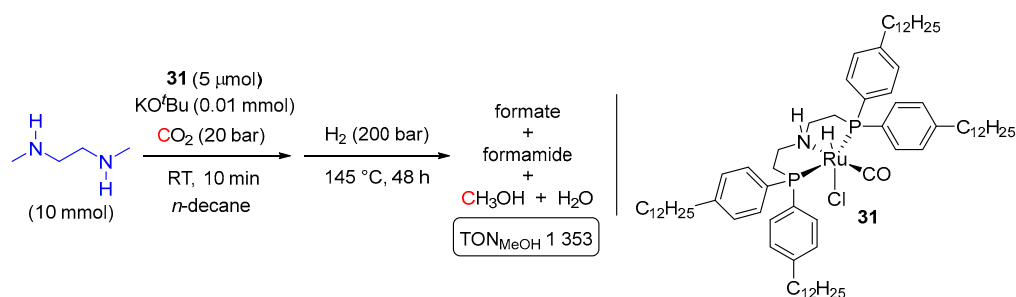
KO^tBu. A temperature ramp from 90 °C to 170 °C and prolonged reaction times (up to 120 h: 48 h at 90 °C and 72 h at 170 °C) were applied and resulted in 84% overall conversion of CO₂ and formation of a mixture of MeOH (TON 2100) and DMF (TON 2070). In addition, **30**-catalyzed hydrogenation of CO₂ to formamides and their further hydrogenation to MeOH were achieved in a stepwise manner. Thus, TONs of 300,000 and 9500 for two separate steps, respectively, were obtained using HNMe₂ for CO₂ trapping (Scheme 15).



Scheme 15. **30**-catalyzed reduction of CO₂ to MeOH in the presence of HNMe₂.

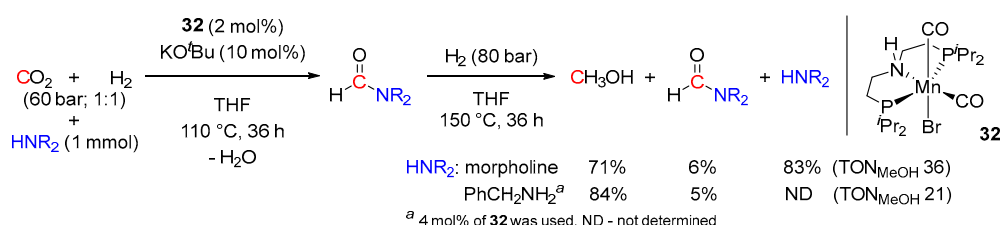
An integrated CO₂ trapping and its sequential reduction to MeOH was also reported in 2019 by the Kayaki group [56]. The catalytic system consisted of (PN^HP)Ru(H)(η^1 -BH₄)(CO) (**23**) and either linear or branched polyethyleneimine (PEI) auxiliaries ($M_n = 600$ –250,000) and allowed production of MeOH without contamination from formate and formamide intermediates. The reactions were conducted in THF in either a sequential or one-pot manner. The latter required heating at above 130 °C and resulted in MeOH production with a TON of 366 using 10 bar of CO₂ (the highest TON of 599 was achieved in 100 h at 150 °C applying 20 bar and 60 bar of CO₂ and H₂, respectively). Interestingly, compared to branched PEI, linear polyamines showed significantly better CO₂ uptake upon the *N*-formylation step (higher CHO content was determined after the reaction due to the absence of inactive tertiary amine linkages); however, the subsequent hydrogenation to methanol was found to be comparatively sluggish. Noteworthy, the use of PEI in **23**-catalyzed CO₂ reduction allowed for convenient separation of MeOH from amines and FA-derived intermediates, which precipitated upon cooling the reaction mixture and could be filtered off.

An example of a self-separating multiphasic system for amine-assisted Ru-catalyzed hydrogenation of CO₂ to MeOH was disclosed by Franciò and Leitner et al. last year [57]. The reaction was conducted in *n*-decane, and the catalyst used resembles complex **23**, originally applied by Sanford et al. (see Scheme 2), but long aliphatic chain substituents were introduced to the ligand to ensure its exclusive partitioning into a non-polar organic solvent (complex **31** in Scheme 16). Here, 1,2-dimethylethylenediamine (DMEDA) was used for CO₂ trapping, and the reaction mixture was first saturated with CO₂ (10 bar) at room temperature. This was followed by heating the mixture under 200 bar of H₂ at 145 °C for 48 h leading to a biphasic liquid-liquid system, from which MeOH can be easily separated with the catalyst remaining in *n*-decane. Although rather harsh hydrogenation conditions were applied, the maximum TON for MeOH of approx. 2000 was obtained, and the developed system allowed for simple catalyst recycling without any significant loss of its activity (total TON_{MeOH} of 19,200 with an average selectivity of 96% over 11 runs).



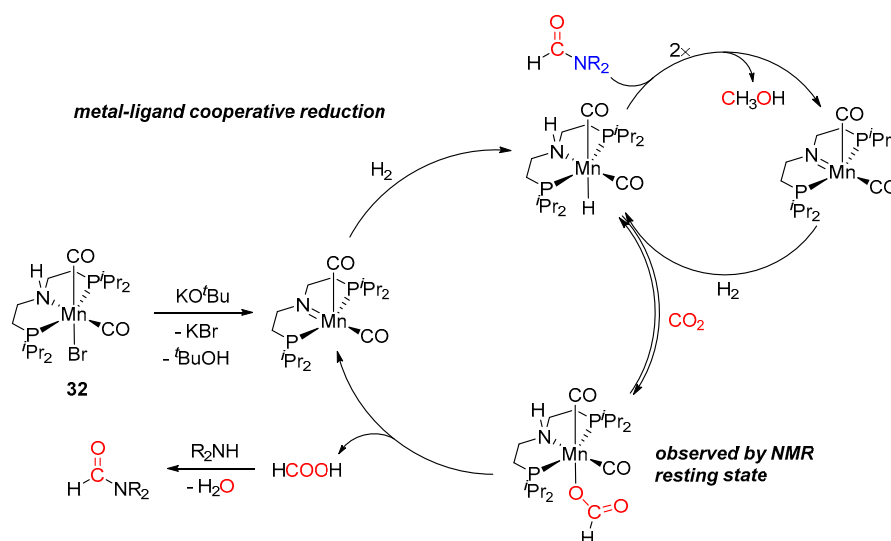
Scheme 16. **31**-catalyzed biphasic reduction of CO₂ to MeOH in the presence of 1,2-dimethylethylenediamine (DMEDA).

Besides ruthenium, several other more economical 3d metal surrogates have been tested in amine-assisted hydrogenation of CO₂ to MeOH [23,58,59], albeit so far these systems generally showed comparatively lower catalytic activities. Thus, by analogy with Ru-PNP catalysts [48,49,51–53], sequential hydrogenation of CO₂ in the presence of aliphatic amines and (PN^HP)Mn(Br)(CO)₂ (**32**) was reported by Prakash et al. in 2017 (Scheme 17) [58]. First, the activity of complex **32** at 2 mol% loading was evaluated in the *N*-formylation of several amines to the corresponding formamides, with the best conversions (93–95% in 24–36 h) observed for morpholine, benzylamine, and *N*-methylbenzylamine. The reactions were performed in THF at 110 °C under 60 bar of CO₂/H₂ (1:1) and were initiated by 10 mol% of KO^tBu as a base. In the next step, the initial CO₂/H₂ pressure was released, and the reaction mixtures were subjected to 70–80 bar of H₂, followed by heating at 150 °C for 24–36 h. A maximum TON of 36 for the two-step conversion of CO₂ to methanol was achieved, which is significantly lower compared to TON values (up to approx. 9000 [54]) observed for analogous Ru-catalyzed transformations (vide supra) [48,49,51–56]. The proposed mechanism of **32**-catalyzed CO₂ reduction is depicted in Scheme 18 and is similar to the pathway suggested for (PN^HP)Ru(H)(η¹-BH₄)(CO) (**23**; Scheme 11 [49]). However, in the case of Mn, the metal-ligand cooperative reactivity of the catalyst was suggested for all steps, including the generation of the formate intermediate.

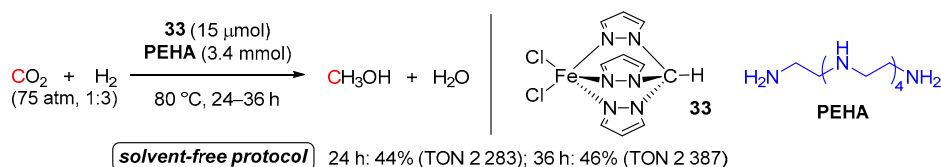


Scheme 17. **32**-catalyzed reduction of CO₂ in the presence of morpholine and benzylamine.

In the same year, Martins and co-workers used the iron(II) scorpionate catalyst FeCl₂{κ³-HC(pz)₃} (**33**; pz = pyrazol-1-yl) for solvent-free hydrogenation of CO₂ to MeOH in the presence of either pentaethylene-hexamine (PEHA) or 1,1,3,3-tetramethyl guanidine (TMG) (Scheme 19) [59]. The maximum yield of MeOH of 46% (TON 2387) was observed with PEHA in 36 h at only 80 °C under 75 atm of CO₂/H₂ (1:3 ratio). High thermal stability of complex **33** allowed for low catalyst loading (only 15 μmol) and a simple constant heating rate, avoiding a “temperature ramp” strategy previously reported for Ru catalysts [48,51,55]. Formation of catalytically active Fe(II) hydride species, akin to Fe(H)(Cl){κ³-HC(pz)₃} and/or FeH₂{κ³-HC(pz)₃}, by either heterolytic H₂ splitting or σ-bond metathesis of H₂ and the Fe-Cl bonds of **33**, was suggested as the reaction initiation step. Noteworthy, complex **33** was also found to mediate the CO₂-to-MeOH reduction using an amine-free protocol.

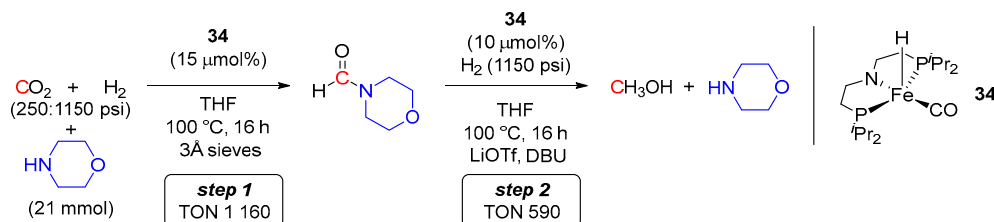


Scheme 18. A plausible mechanism for **32**/amine-catalyzed hydrogenation of CO₂ to MeOH.



Scheme 19. **33**/pentaethylene-hexamine-catalyzed reduction of CO₂ to MeOH.

A more recent example of an iron catalyst for sequential amine-assisted hydrogenation of CO₂ to MeOH via the formamide intermediate was reported by Bernskoetter et al. [23]. By analogy with Ru-PNP and Mn-PNP derivatives, (PNP)Fe(H)(CO) (**34**) was employed as a catalyst, and hydrogenation of CO₂ was achieved in a two-step manner (Scheme 20). In the first step, using morpholine as a shuttle and conducting the reaction at 100 °C with CO₂/H₂ (250/1150 psi) resulted in 83% conversion of CO₂ to *N*-formyl-morpholine with a TON of 1160. The second formamide hydrogenation step was also conducted at 100 °C using 1150 psi of H₂ and showed a maximum TON of 590 for MeOH. The catalyst **34** was added at both steps of the transformation. Importantly, completion of the first formylation step required the addition of 3 Å molecular sieves to avoid catalyst deactivation by water generated in situ, whereas the addition of LiOTf and DBU was required in the second hydrogenation step to avoid the formation of ammonium carbamates, which seem to inhibit the production of MeOH. Moreover, similarly to the Mn-PNP system reported previously by Parkash et al. [58], complex **34** was unable to convert CO₂ to MeOH in a single-step manner. Large excess CO₂ was required to produce the formamide intermediate but inhibited its turnover to MeOH, presumably due to the formation of the stable [Fe-OC(O)H] resting state [60], decarboxylation of which, to produce catalytically active Fe-H species, was suppressed by the excess of CO₂.

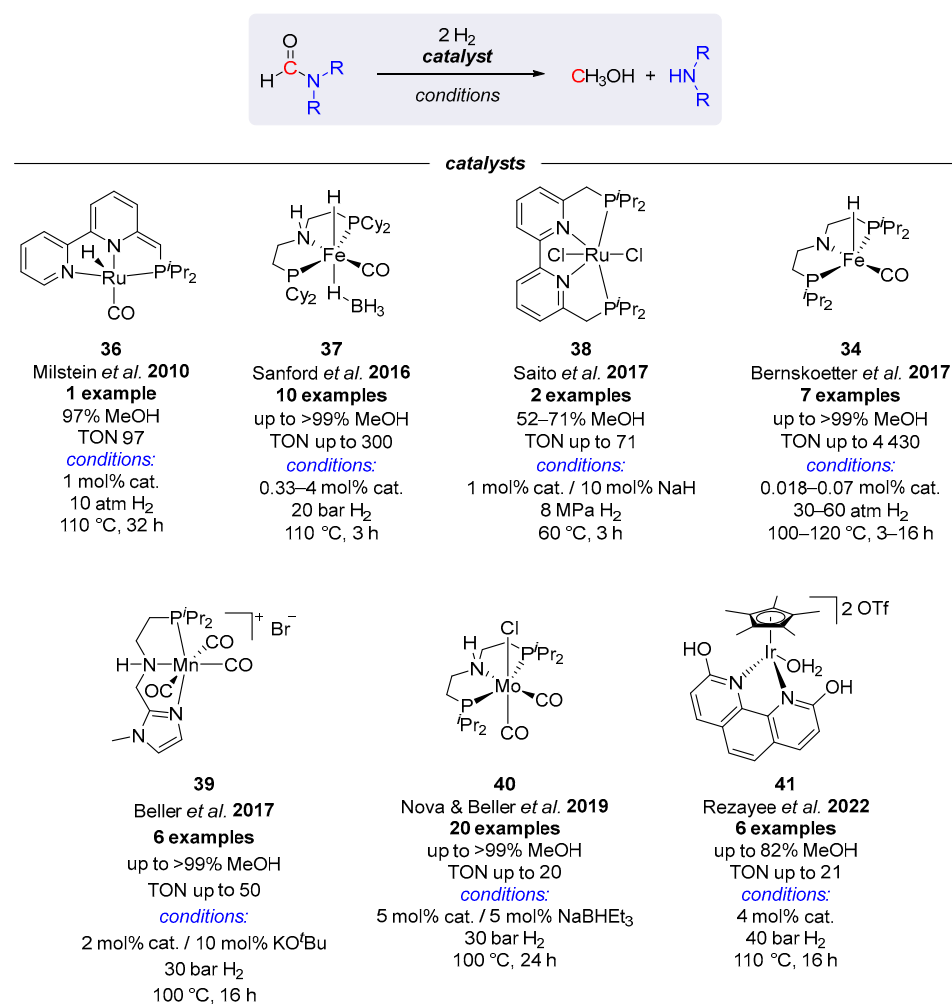


Scheme 20. **34**/morpholine-catalyzed two-step reduction of CO₂ to MeOH.

Noteworthy, the related iron complex (PN^HP)Fe(H)(η^1 -BH₄)(CO) (**35**) has been recently disclosed by Junge, Du, and Beller et al. as a catalyst for formamide-based hydrogen

storage and release cycles [61]. Although no production of MeOH was reported, complex **35** was found active in the amine-assisted hydrogenation of CO₂ to formamides, as well as in catalytic dehydrogenation of formamides, and the system demonstrated high H₂ charge-discharge capacity over 10 consecutive cycles.

Apart from sequential routes to methanol from CO₂ and amines, in which formamides are produced as reaction intermediates, several transition metal complexes have been reported to mediate the production of MeOH from formamides without participation in their formation via *N*-formylation reactions [62–68]. The best-performing systems for such hydrogenolysis of formamides are summarized in Scheme 21. From these, the highest TON for MeOH was detected for complex **34** [65], and others were found significantly less active. Notably, the ruthenium complex **38** was found to mediate the hydrogenolysis of formamides even at 60 °C within 3 h, which represents a rare example of a catalytic system for mild production of MeOH from CO₂ derivatives [64]. It is also noteworthy that **38** was applied in tandem hydrogenation of CO₂ to MeOH in the presence of HNMe₂ (yield 52%), where RuCl₂(PMe₃)₄ was utilized in the first *N*-formylation step [64].



Scheme 21. Transition metal complexes studied in the hydrogenation of formamides to MeOH [62–68].

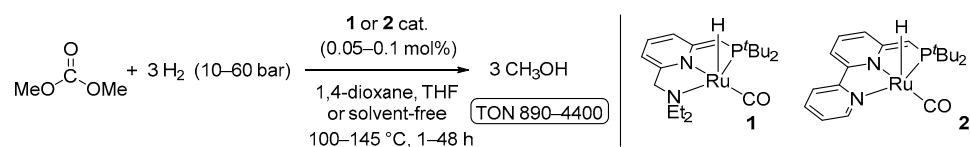
4. Catalytic Hydrogenation of Carbonates

Organic carbonates are widespread chemicals in industrial synthetic chemistry. They find applications in many different areas, including but not limited to pharmaceuticals, agrochemicals, lubricants, polymers, electrolytes, etc. [27]. They are also widely used as “green” solvents due to their low toxicity [28,69,70]. Conventionally, organic carbonates are produced by phosgenation of alcohols or by catalytic oxidative carbonylation of alcohols; however, a significant shift towards CO₂-based processes for the production of organic

carbonates has been seen in recent decades [29,69–72]. Considering the advances in these technologies as well as the constantly growing industrial demand for organic carbonates (produced on a scale of several 100 kilotons per year) [29], production of MeOH by hydrogenation of CO₂-derived carbonates represents an attractive alternative to direct CO₂ reduction [34]. Nonetheless, the hydrogenation of organic carbonates remains a challenging task due to their low electrophilicity. The following discussion is devoted to developments in homogeneous transition metal-catalyzed hydrogenation of linear organic carbonates, cyclic organic carbonates, and some tandem approaches via carbonate salts to methanol.

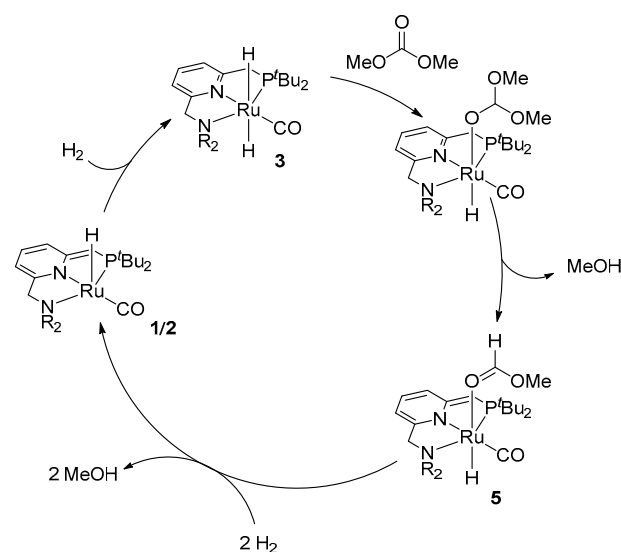
4.1. Hydrogenation of Acyclic Organic Carbonates

The first example of homogeneous catalytic hydrogenation of dimethyl carbonate along with other CO₂ derivatives (such as formates and carbamates) was reported by Milstein in 2011 using Ru-PNN pincer complexes **1** and **2** (Scheme 22) [34]. The reactions were tested in either 1,4-dioxane or THF at 10–60 bar of H₂ and 100–145 °C. The maximum TON of 4400 for methanol was achieved using only 0.05 mol% of the catalyst **2** and conducting the hydrogenation at 50 bar of H₂ and 110 °C for 14 h. Remarkably, **2**-catalyzed reduction of Me₂CO₃ to MeOH with TON > 990 was also performed using only 10 bar of H₂ under neat conditions.



Scheme 22. Ru PNN-catalyzed hydrogenation of dimethyl carbonate to MeOH.

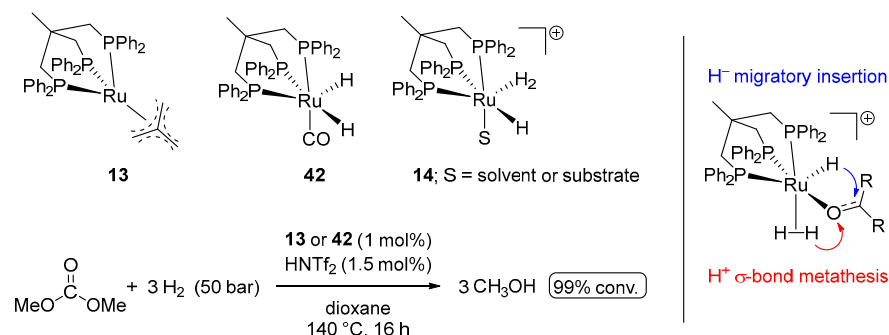
The reduction of dimethyl carbonate catalyzed by complexes **1** and **2** was proposed to proceed via an MLC mechanism (Scheme 23) with an intermediacy of methyl formate [34,35]. The reaction is initiated by the heterolytic cleavage of H₂ by the amide catalysts **1** and **2** to give a dihydride intermediate **3**. This is followed by the migratory insertion of the carbonate to the Ru–H bond, the release of a molecule of MeOH, and the formation of the methyl formate complex **5**. The latter intermediate reacts with two more equivalents of H₂ to recover the catalyst and produce two more equivalents of methanol, according to Scheme 3 above.



Scheme 23. A plausible mechanism for Ru PNN-catalyzed hydrogenation of dimethyl carbonate to MeOH.

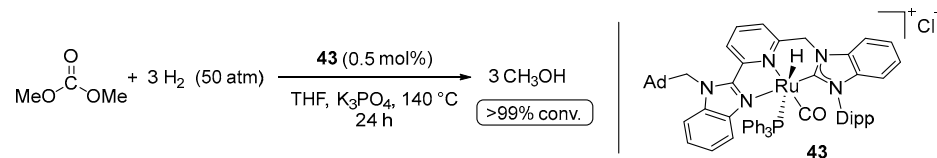
In 2014, Klankermayer and Leitner et al. also demonstrated the hydrogenation of dimethyl carbonate to methanol using Ru Triphos pre-catalysts **13** and **42** (Scheme 24) [73].

Similarly to **13**-catalyzed EtOH-assisted hydrogenation of CO₂ to MeOH, the reactions required activation with HNTf₂ to generate the catalytically active cationic Ru(II) species **14** [74], amenable to the proton transfer from the dihydrogen ligand to the carbonyl group (Scheme 24).



Scheme 24. (Triphos)Ru complexes for hydrogenation of dimethyl carbonate to MeOH.

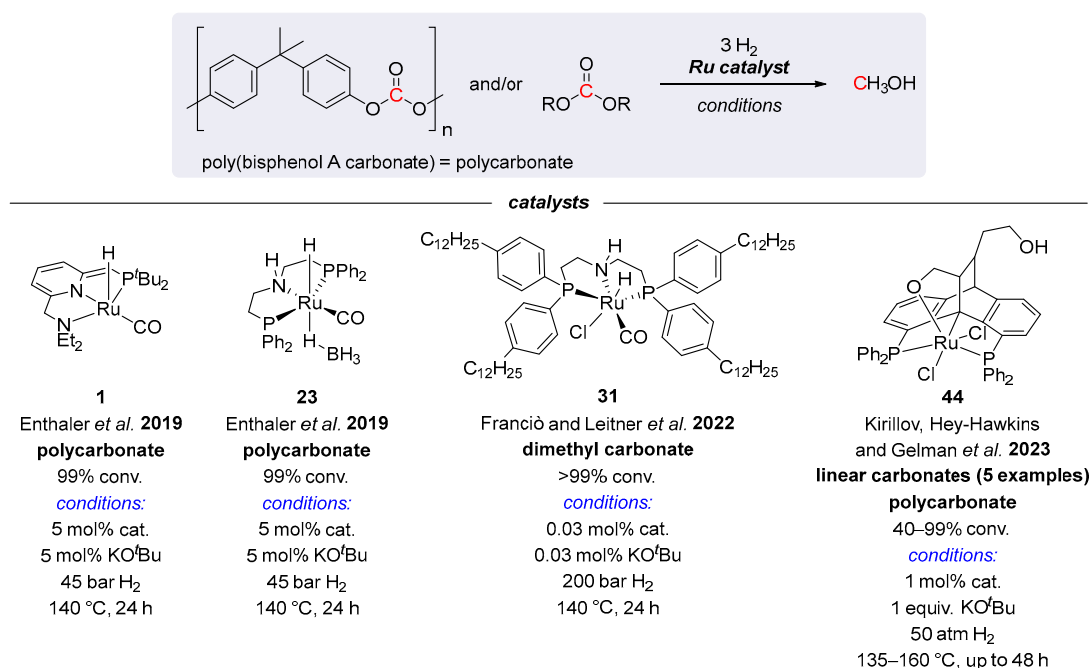
Yet another Ru(II) pre-catalyst **43** for the hydrogenation of dimethyl carbonate to methanol was reported by Chen et al. in 2017 (Scheme 25) [75]. The system resembled the Milstein-type catalysts **1–4** [34], where the phosphine side-arm of the ligand is replaced with the *N*-heterocyclic carbene (NHC) donor. The reduction of dimethyl carbonate was conducted with 50 bar of H₂ at 140 °C using 0.5 mol% of **43** activated with K₃PO₄ and resulted in >99% conversion to MeOH within 24 h. The same system was also found to be highly active in the hydrogenation of cyclic carbonates (vide infra). The suggested mechanism likely involves base-assisted dearomatization of the pyridine ligand following the general scheme proposed previously by Milstein et al. (see Scheme 23) [34].



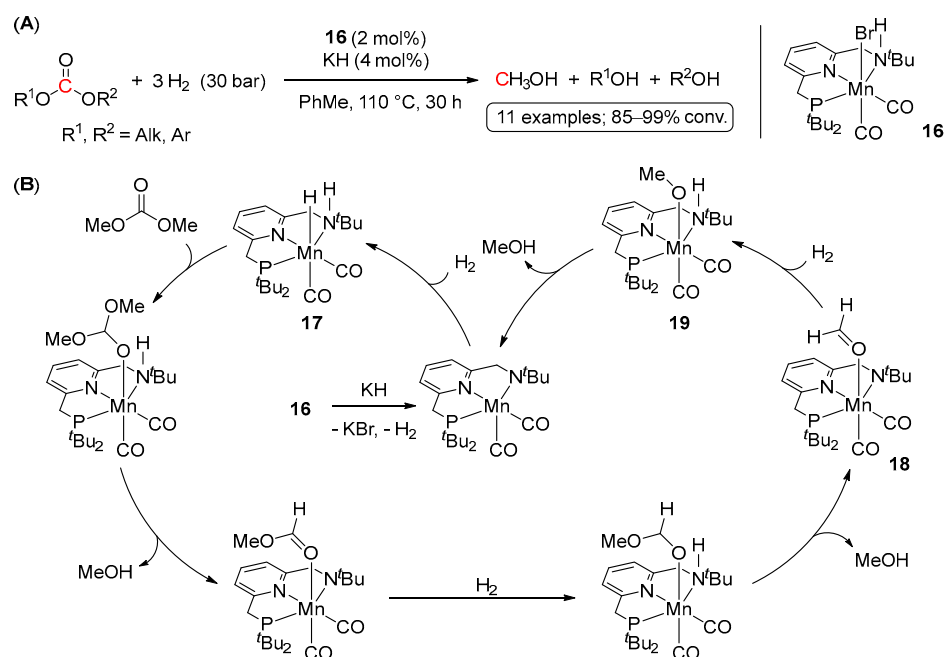
Scheme 25. **43**-catalyzed hydrogenation of dimethyl carbonate to MeOH.

Since 2017, several other examples of Ru-catalyzed hydrogenations of linear carbonates and polycarbonates have been reported [57,76–78]. These systems are summarized in Scheme 26, and all operate via MLC pathways. Thus, complexes **1**, **23**, and **44** were applied in hydrogenative depolymerization of a bisphenol A-derived polycarbonate, routinely used in protective CD/DVD films [76–78]. The reactions afforded MeOH and bisphenol A as the products of the carbonate linkage cleavage, although rather large quantities of KO^{*t*}Bu (1 equiv.) were required in the **44**-catalyzed reaction. On the other hand, the use of the lipophilic PNP derivative **31** in the hydrogenation of dimethyl carbonate in *n*-decane allowed for efficient catalyst separation and reuse. Although the reactions were conducted with only 0.03 mol% loading of **31**, high H₂ pressure of 200 bar was required to fully convert Me₂CO₃ to MeOH [57].

Moving away from ruthenium systems, in 2018 Milstein et al. reported on Mn-catalyzed hydrogenation of carbonates [42]. Applying a bifunctional Mn(I) PNN pre-catalyst, (PNN^H)Mn(Br)(CO)₂ (**16**), a variety of symmetrical and unsymmetrical acyclic carbonates were hydrogenated to the corresponding alcohols and methanol with excellent conversions under relatively mild conditions (110 °C, 30 bar of H₂) (Scheme 27A). Moreover, hydrogenative depolymerization of poly(propylene carbonate) was also demonstrated, suggesting the applicability of the system for polycarbonate waste treatment. The proposed reaction mechanism is depicted in Scheme 27B and involves a nonoxidative metal–ligand cooperative pathway between the Mn center and the secondary amine functionality of the side arm of the ligand.

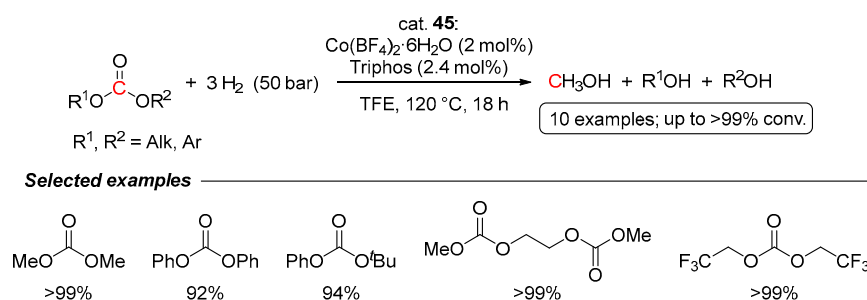


Scheme 26. Ru complexes for hydrogenation of acyclic carbonates and polycarbonates [57,76–78].



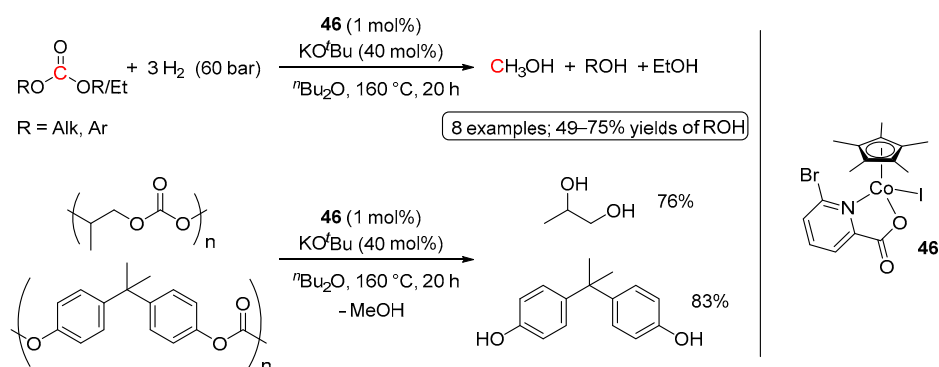
Scheme 27. (A) Hydrogenation of Me₂CO₃ to MeOH catalyzed by Mn(I) complex **16**; (B) a plausible metal–ligand cooperative mechanism for **16**-catalyzed hydrogenation of methyl carbonate.

The first example of cobalt-catalyzed hydrogenation of carbonates has been recently demonstrated by Beller and co-workers [79]. A series of commercially available Co(II) and Co(III) salts and polydentate phosphine ligands have been tested, with Co(BF₄)₂·6H₂O/Triphos (**45**) being the most active. Several symmetric and non-symmetric acyclic carbonates were efficiently hydrogenated to MeOH and the corresponding alcohols using 2 mol% of Co loading and 50 bar of H₂. Almost quantitative conversions were achieved in 2,2,2-trifluoroethanol (TFE) at relatively mild and additive-free conditions (120 °C, 18 h; Scheme 28). Similarly to previous reports on the hydrogenation of linear carbonates, the reactions were proposed to proceed via formate and formaldehyde intermediates.



Scheme 28. Co(BF₄)₂·6H₂O/Triphos (**45**)-catalyzed hydrogenation of acyclic carbonates.

Another cobalt catalyst for the hydrogenation of acyclic carbonates and polycarbonates has been disclosed by Sundararaju et al. in 2021 [80]. The system comprised of a [Cp*Co(I)(pyridine-2-carboxylate)] complex **46**, activated with KO^tBu (Scheme 29). The reactions were performed in ⁿBu₂O at 160 °C for 20 h; however, rather large quantities of KO^tBu were required (40 mol%). Nonetheless, along with acyclic monomeric carbonates, hydrogenative depolymerization of polycarbonates, such as poly(propylene carbonate), and poly(bisphenol A carbonate), was demonstrated, suggesting the practical utility of the system in polymer recycling.



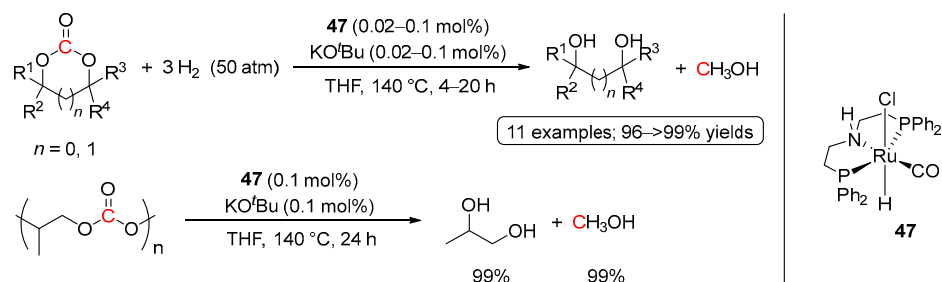
Scheme 29. **46**-catalyzed hydrogenation of acyclic carbonates and polycarbonates.

4.2. Hydrogenation of Cyclic Organic Carbonates

Compared to linear organic carbonates, cyclic carbonates are relatively easily accessible based on the treatment of readily available oxiranes (such as ethylene or propylene oxides) with CO₂. The driving force for this transformation is the high energy content of the oxirane molecule, and different catalysts have been developed for this transformation to provide cyclic carbonates with good to excellent yields [29]. Alternatively, cyclic carbonates can also be produced in good yields by the reaction of CO₂ with 1,2- and/or 1,3-diols; however, the presence of a water-trapping agent is required to shift the equilibrium towards the carbonate product [29]. The subsequent hydrogenation of cyclic carbonates results in the formation of MeOH and the recovery of a diol, and the overall sequence represents an attractive approach for the conversion of CO₂ to MeOH.

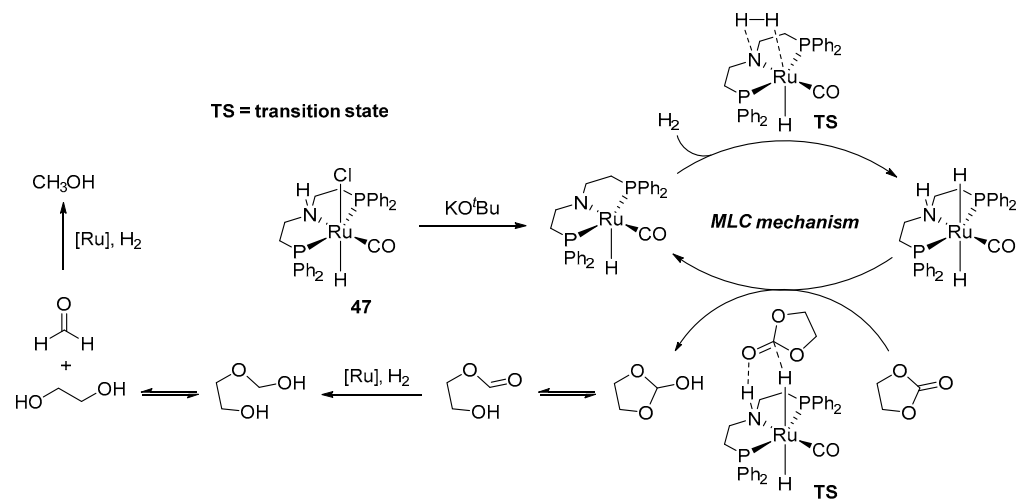
To the best of our knowledge, homogeneous hydrogenation of cyclic carbonates was disclosed for the first time by Ding and co-workers in 2012 [81]. Despite previously reported successful application of Ru(II)-PNN complexes in the hydrogenation of dimethyl carbonate by Milstein et al. (see Scheme 22) [34], hydrogenation of ethylene carbonate to MeOH and ethylene glycol (EG) represents a more economically appealing approach for utilization of CO₂, since the production of ethylene carbonate from CO₂ and ethylene oxide is a thermodynamically favorable process. Moreover, the industrial synthesis of ethylene carbonate has been well-developed as a part of the “omega process” for the production of EG, with global demands of >25 million metric tons per year (used as a precursor to polyester and as a component in automotive antifreeze) [81]. With this in mind, the catalytic activity of Ru(II) pincer systems was tested in the hydrogenation of a

series of cyclic organic carbonates, with the best conversions to MeOH and diols achieved for $(\text{PN}^{\text{H}}\text{P})\text{Ru}(\text{H})(\text{Cl})(\text{CO})$ (**47**; Scheme 30). The reactions were conducted in THF at 140 °C using 50 bar of H_2 and rather low loadings of **47** (0.02–0.1 mol%) and showed almost quantitative yields of the alcohol products (96–>99%). The high efficiency of **47**, as well as its high stability, was demonstrated by hydrogenation of ethylene carbonate at 0.001 mol% catalyst loading, resulting in 72 h at 140 °C in 84% and 87% of MeOH and EG, respectively, with a TON of 87,000 and a TOF of 1200 h^{-1} . Moreover, the same system was found to be highly active in hydrogenative depolymerization of poly(propylene carbonate) conducted on a several grams scale with only 0.1 mol% of the catalyst loading (Scheme 30).



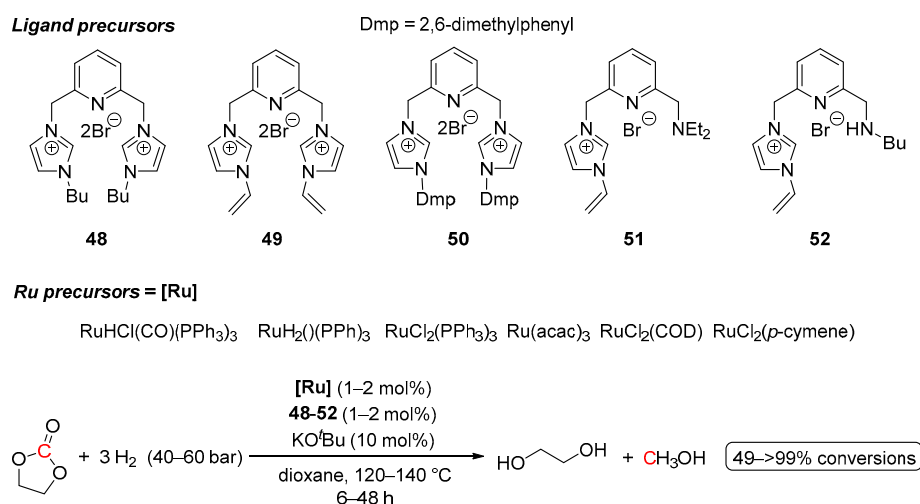
Scheme 30. **47**-catalyzed hydrogenation of cyclic carbonates and polycarbonates.

A plausible mechanism of **47**-catalyzed hydrogenation of ethylene carbonate is shown in Scheme 31. The reaction was proposed to proceed via an outer-sphere MLC pathway, which is initiated by the treatment of **46** with KO^tBu to generate the catalytically active Ru(II) amide species. This is followed by the heterolytic cleavage of H_2 and the concerted proton/hydride transfer to the carbonyl group of first carbonate, then formate, and, finally, formaldehyde, as depicted in Scheme 31.



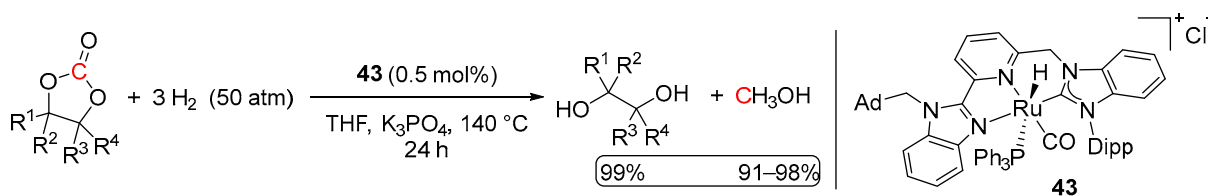
Scheme 31. Proposed MLC mechanism of **47**-catalyzed hydrogenation of ethylene carbonate.

Driven by the idea of designing more robust phosphine-free Ru(II) pre-catalysts for the hydrogenation of cyclic carbonates, in 2016 Gao et al. reported the hydrogenation of ethylene carbonate, catalyzed by commercial Ru precursors, ligated with lutidine-bridged NHC ligands (Scheme 32) [82]. Among all the tested ligands and Ru precursors, $\text{RuHCl}(\text{CO})(\text{PPh}_3)_3$ in combination with the ligand **48** was found to be the most efficient, resulting in >99% conversion of ethylene carbonate and 92% and 42% yields of glycol and MeOH, respectively. However, overall, these systems turned out to be less active compared to the analogous Ru-PNP catalyst **47**.



Scheme 32. Ru-NHC-catalyzed hydrogenation of ethylene carbonate.

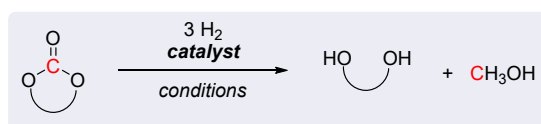
Significantly more efficient hydrogenation of cyclic carbonates using Ru-NHC complex **43** has been reported by Chen et al. [75]. Despite the sterically hindered nature of **43**, nearly quantitative conversions of cyclic carbonates to MeOH and the corresponding diols were observed under 50 atm of H₂, 140 °C, and only 0.5 mol% of Ru loading (Scheme 33). Noteworthy, compared to systems **48–52**, which required the use of a strongly basic KO^tBu, activation of **43**-catalyzed reactions was achieved with K₃PO₄. The initiation step was suggested to proceed via dearomatization of the bridgehead pyridine moiety, resulting in a Milstein-type MLC mechanism [34,35].



Scheme 33. **43**-catalyzed hydrogenation of cyclic carbonates.

Concerning other Ru systems, the hydrogenation of ethylene and propylene carbonates has also been demonstrated using a high-valent (PCP)Ru^{IV} complex **44** (Scheme 26) [78]. Although nearly quantitative yields of MeOH (94–98%), ethylene glycol (99%), and propylene glycol (99%) were detected in 20 h at 1 mol% loading of **44**, 50 atm of H₂ and 130 °C, the reactions required stoichiometric amounts of KO^tBu, presenting a significant drawback of the system compared to other Ru catalysts.

Apart from Ru catalysts, in a general trend to develop more economical surrogates for precious metal systems, several manganese [42,83,84] and cobalt complexes [79,80] have been shown to catalyze the hydrogenation of cyclic carbonates (Scheme 34). However, despite the observed high conversions to MeOH and the corresponding diols, these base metal systems are still inferior to the catalytic activity of the ruthenium complex **47**.

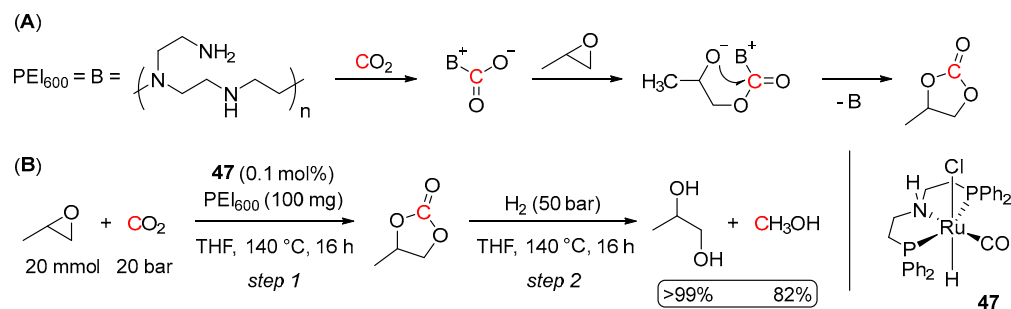


catalysts

<p>16 Milstein <i>et al.</i> 2018 3 examples 94–99% conv. <i>conditions:</i> 2 mol% cat. 4 mol% KH 50 bar H₂ 110 °C, 50 h</p>	<p>32 Leitner <i>et al.</i> 2018 7 examples 77→99% conv. <i>conditions:</i> 2 mol% cat. 2.2 mol% NaO^tBu 30 bar H₂ 120 °C, 26 h</p>	<p>53 Cavallo, El-Sepelgy, Rueping <i>et al.</i> 2018 12 examples 94–99% yields of diols <i>conditions:</i> 1 mol% cat. 2.5 mol% KO^tBu 50 bar H₂ 140 °C, 16 h</p>	<p>45 Beller <i>et al.</i> 2019 5 examples >99% conv. <i>conditions:</i> 2 mol% cat. 2.4 mol% ligand 50 bar H₂ 120 °C, 18 h</p>	<p>46 Sundararaju <i>et al.</i> 2021 11 examples 82–92% yields of diols <i>conditions:</i> 1 mol% cat. 40 mol% KO^tBu 60 bar H₂ 160 °C, 20 h</p>
--	--	---	---	---

Scheme 34. Base metal complexes for hydrogenation of cyclic carbonates [42,79,80,83,84].

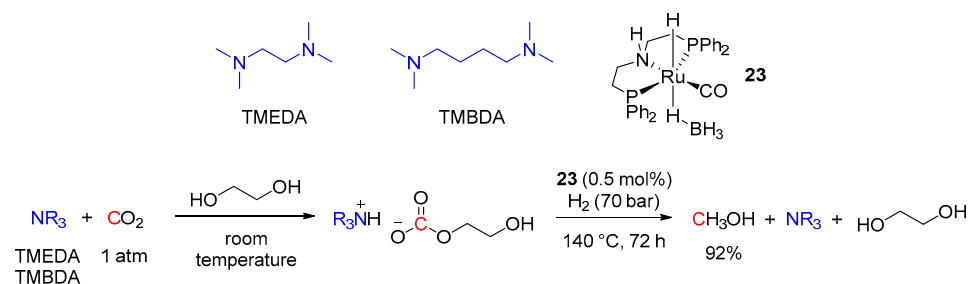
Finally, the feasibility of a one-pot strategy for the coproduction of MeOH and propylene glycol from CO₂, propylene oxide, and H₂ has been recently demonstrated by Heldebrant *et al.* [85]. The overall transformation consisted of two steps: the formation of propylene carbonate from the epoxide and CO₂ and further hydrogenation of the carbonate to MeOH and the glycol. Considering the ability of amines and amino alcohols to capture CO₂ and promote its further hydrogenation to formates and methanol [86–89], the first step, the reaction of CO₂ with propylene oxide, was achieved using branched polyethyleneimine (PEI₆₀₀) as a catalyst. Herein, PEI₆₀₀ is suggested to activate CO₂ allowing for nucleophilic attack of the carbanion on the epoxide, leading to ring-opening of the epoxide, followed by cyclization to the carbonate (Scheme 35A). The following hydrogenation step was tested with a series of Ru catalysts, among which the best performance was demonstrated for (PN^HP)Ru(H)(Cl)(CO) (**47**). The overall transformation was conducted in a sequential one-pot manner in THF at 140 °C with 20 bar of CO₂ and 50 bar of H₂ and only 0.1 mol% of **47** and resulted in >99% yield of the propylene glycol and 24% yield of MeOH (Scheme 35B). Noteworthy, to avoid disassembly of the pressurized reactor after the first step, the Ru catalyst was added to the system right away along with the propylene oxide, CO₂, and PEI₆₀₀. The H₂ gas was introduced only after the completion of the first step. This, however, did not affect the rate of the carbonate formation and the overall reaction outcome, suggesting no deactivation of the Ru catalyst in the presence of CO₂.



Scheme 35. (A) CO₂ capture with PEI₆₀₀; (B) One-pot production of MeOH and propylene glycol from CO₂, propylene oxide, and H₂.

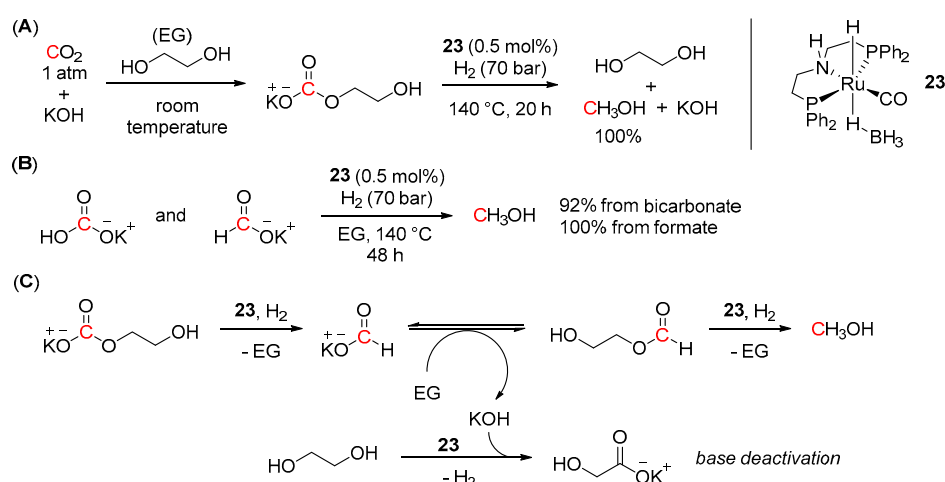
4.3. Hydrogenation of Carbonate Salts

Although the use of primary and secondary amines in CO₂ capture and hydrogenation via formamide intermediates has been extensively investigated (see Section 3) [48–68], utilization of tertiary amines as CO₂ scrubbing agents in CO₂-to-MeOH reduction is underdeveloped [86–88,90]. Tertiary amines are incapable of generation of formamides, and trapping CO₂ with tertiary amine–alcohol mixtures leads to the production of ammonium carbonates, which further undergo hydrogenation to methanol. The first examples of such a tandem approach to MeOH using tertiary amine–alcohol mixtures for CO₂ trapping was demonstrated by Heldebrant et al. using Cu/ZnO/Al₂O₃ as a heterogeneous catalyst under rather harsh reaction conditions (temperatures of 170 °C and above) [86,88]. Shortly after, Prakash et al. adopted this methodology to homogeneously catalyzed reduction of CO₂ to MeOH using the Ru-PNP complex **23** [90]. The reactions were conducted in ethylene glycol (EG), and several tertiary amines (such as tetramethyl-ethylenediamine (TMEDA), tetramethyl-1,4-butanediamine (TMBDA), triethanolamine (TEA), pentamethyl-diethylenetriamine (PMDETA) and others) were tested. The most efficient formation of MeOH was observed for TMEDA and TMBDA (92% yield for both). The overall transformation of CO₂ to MeOH was performed in a sequential manner, where the first CO₂ capture step was achieved within 3 h at ambient temperature and atmospheric pressure, followed by the **23**-catalyzed (0.5 mol%) hydrogenation step at 140 °C and 70 bar of H₂ (Scheme 36). The possibility of amine recycling and reuse for subsequent CO₂ capture was also demonstrated. In addition, the system showed efficient CO₂ capture from synthetic flue gas (10% CO₂ in N₂) and its effective conversion to MeOH (72% and 94% yields for TMEDA and TMBDA, respectively), showing potential direct utilization of post-combustion CO₂.



Scheme 36. Tertiary amine–ethylene glycol based tandem CO₂ capture and hydrogenation to MeOH.

A similar approach via CO₂ capture in the form of carbonate salts has also been tested using alkali hydroxides. Thus, quantitative conversion of CO₂ to MeOH (TON 200) was reported by Prakash and co-workers using 0.5 mol% of complex **23** and 0.5 M solution of KOH in ethylene glycol as the CO₂ trapping agent [91]. Analogously to tertiary amines, the reaction was performed in a sequential one-pot manner. The CO₂ capture step was achieved within 3 h at room temperature and atmospheric pressure, whereas the following hydrogenation reaction required 70 bar of H₂, 140 °C, and 20 h for completion (Scheme 37A). In addition, excellent yields of MeOH (92% and 100%) were also detected upon **23**-catalyzed hydrogenation of potassium bicarbonate and potassium formate, respectively (Scheme 37B). Remarkably, the system also proved effective in direct CO₂ capture from the air and its further quantitative conversion to methanol, albeit longer times were required for both CO₂ capture and reduction steps (48 and 72 h, respectively). The suggested hydrogenation reaction pathway is depicted in Scheme 37C and includes a **23**-catalyzed formation of potassium formate and its further esterification to alkyl formate, which then undergoes hydrogenation to MeOH. Despite the observed high efficacy of the developed KOH/EG/Ru system in CO₂ capture and hydrogenation to methanol, the main issue of this approach was related to the deactivation of the base with ethylene glycol to give potassium glycolate salts (Scheme 37C), hindering regeneration and reuse of the base.

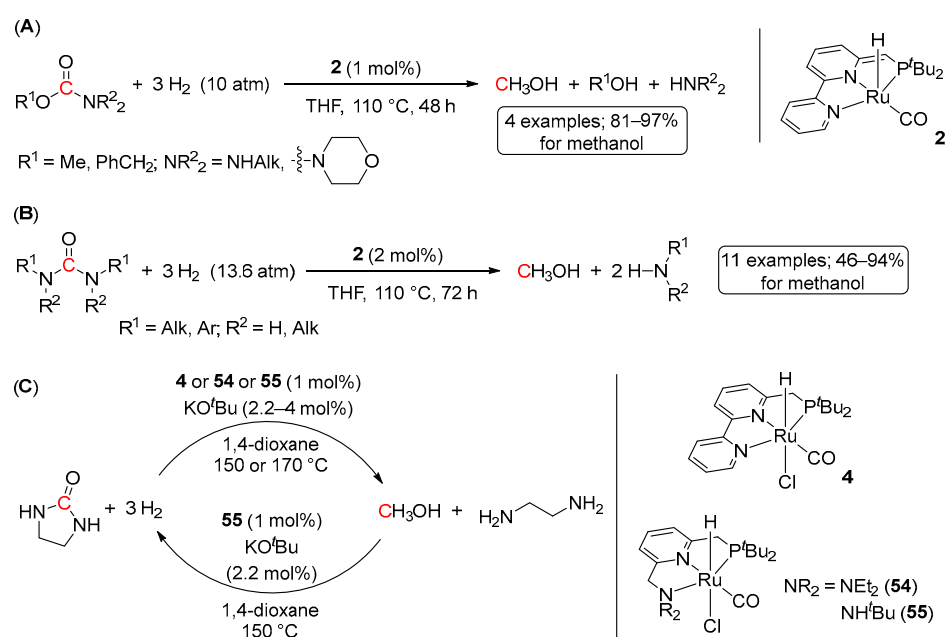


Scheme 37. (A) KOH—ethylene glycol-based tandem CO₂ capture and hydrogenation to MeOH; (B) **23**-catalyzed hydrogenation of potassium bicarbonate and potassium formate; (C) proposed reaction pathway for **23**-catalyzed hydrogenation of potassium carbonate.

5. Catalytic Hydrogenation of Carbamates and Urea Derivatives

Carbamates and ureas, having a relatively less electrophilic carbonyl group, are the most challenging derivatives to undergo hydrogenation [92]. Moreover, there are reports on catalytic hydrogenation reactions where ureas were used as solvents, being considered inert to hydrogenation [93,94]. Therefore, examples of hydrogenation of carbamate and urea derivatives are rather scarce.

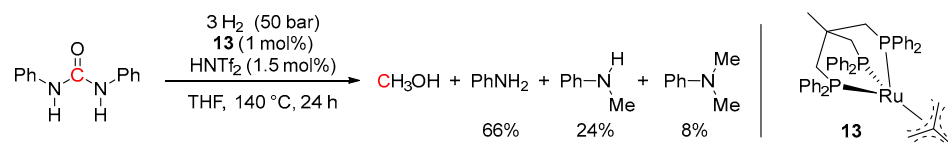
Probably the first instance of homogeneously catalyzed hydrogenation of carbamates was reported in 2011 by Milstein et al. using a (PNN)Ru(II) complex **2** [34]. The reactions were performed at 110 °C for 48 h at 1 mol% of the catalyst loading and only 10 bar of H₂ (Scheme 38A). Methyl carbamates were quantitatively converted to MeOH and the corresponding amines, whereas benzyl carbamates afforded MeOH, the corresponding amines, and benzyl alcohol. Remarkably, in the latter case, no benzyl-O bond cleavage was detected, which contrasts with Pd/C-catalyzed hydrogenolysis of benzyl carbamates used for deprotection of carbamate-*N* functional groups via the release of CO₂ [95].



Scheme 38. **2**-catalyzed hydrogenation of carbamates (A) and urea derivatives (B), and a reversible liquid organic hydrogen carrier system based on methanol-ethylenediamine and ethyl urea (C).

Analogously to carbamates, complex **2** was also reported to catalyze the hydrogenation of urea derivatives [96]. The reactions required 2 mol% loading of the catalyst and 72 h at 110 °C to afford moderate to high yields of MeOH (58–94%) and the corresponding amines for both alkyl and aryl disubstituted urea derivatives (Scheme 38B). More sterically hindered tetra-substituted ureas showed somewhat lower conversions (46–63%). Notably, trace amounts of formamides were also detected in the latter reactions, suggesting a stepwise hydrogenation pathway, in which urea derivatives first undergo conversions to formamides, followed by their hydrogenation to methanol. The observed catalytic activity of Ru-PNN complexes has resulted in the development of a reversible liquid organic hydrogen carrier system, which is based on Ru-catalyzed hydrogenation of the ethylene urea to methanol and ethylenediamine and the reverse process, Ru-catalyzed dehydrogenative coupling of ethylenediamine and MeOH to ethylene urea (Scheme 38C) [97].

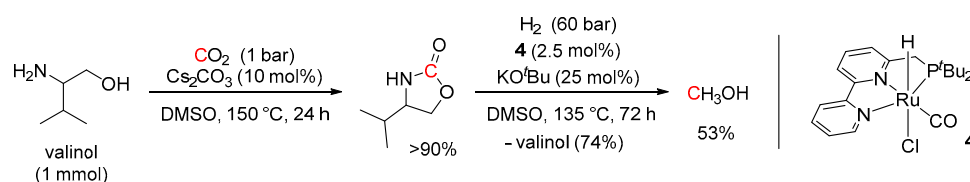
In 2014, Klankermayer and Leitner et al. demonstrated the use of the Ru-Triphos pre-catalyst **13** in the acid-co-catalyzed hydrogenation of 1,3-diphenylurea [73]. The reaction was performed in THF at 140 °C and 50 bar of H₂ using 1 mol% of **13** and 1.5 mol% of HNTf₂ (Scheme 39). After 24 h, 98% conversion of 1,3-diphenylurea was observed; however, a mixture of amine products was obtained (66% of aniline, 24% of methyl aniline, 8% of dimethylaniline). Without HNTf₂, the analogous **13**-catalyzed hydrogenation of 1,3-diphenylurea resulted in selective cleavage of only one C-N bond to yield aniline (75%) and *N*-phenyl formamide (74%). Such dependence of the selectivity of the reaction on the presence of HNTf₂ additive was rationalized by the acid-assisted formation of a cationic species [Ru(Triphos)(Solvent)(H)(H₂)]⁺ (**14**, vs. neutral hydride **41**; Scheme 24), which likely provides better stability of the system at high temperatures.



Scheme 39. **13**/HNTf₂-catalyzed hydrogenation of 1,3-diphenylurea.

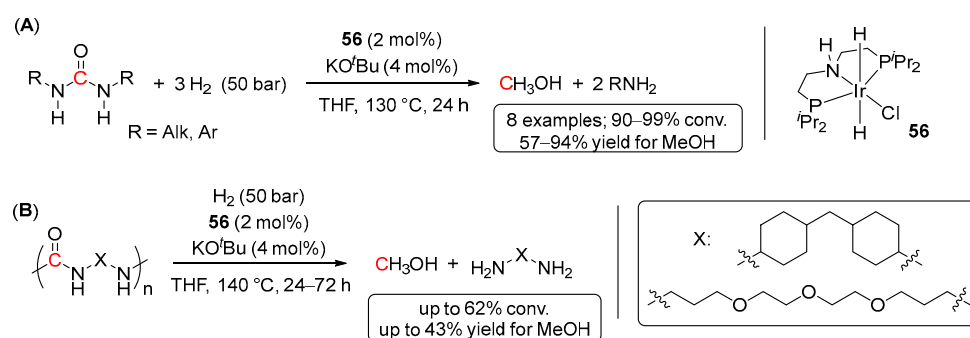
The formation of carbamates and their further hydrogenation to methanol has been also proposed by Prakash et al. during the tandem CO₂ capture/hydrogenation using pentaethylene-hexamine (PEHA) and (PN^HP)Ru(H)(BH₄)(CO) (**23**; Scheme 13) [53]. The capture of CO₂ with an aqueous solution of PEHA (0.33 g/mL) resulted in the formation of a mixture of a carbamate intermediate with bicarbonate/carbonates. This mixture was further subjected to **23**-catalyzed hydrogenation with 80 bar of H₂ to give a 95% yield of MeOH after 72 h at 145 °C. The proposed mechanism for this transformation is described in Section 3 (Scheme 13A) and includes hydrogenation of the carbamate intermediate to afford ammonium formate, which is then converted to the formamide species and finally to methanol.

A similar combination of CO₂ capture and hydrogenation to MeOH has been demonstrated by Milstein et al. using amino-alcohols as low-pressure CO₂ capture reagents and Ru complex **4** as a hydrogenation pre-catalyst [98]. The overall transformation of CO₂ to MeOH was performed in two steps. The best results for the CO₂ capture step were achieved with valinol using only 1 bar of CO₂ and 10 mol% of Cs₂CO₃ as a base to give 4-isopropyl-2-oxazolidinone in >90% yield after 24 h at 150 °C (Scheme 40). The next hydrogenation step was performed using 2.5 mol% of the pre-catalyst **4**, 25 mol% of KO^tBu as a base, and 60 bar of H₂ and resulted in 53% of MeOH and 74% recovery of valinol after 72 h at 135 °C. The advantage of the developed approach is in the direct conversion of the CO₂ capture products to MeOH without isolation of the intermediates and the need for energetically expensive decarboxylation processes.



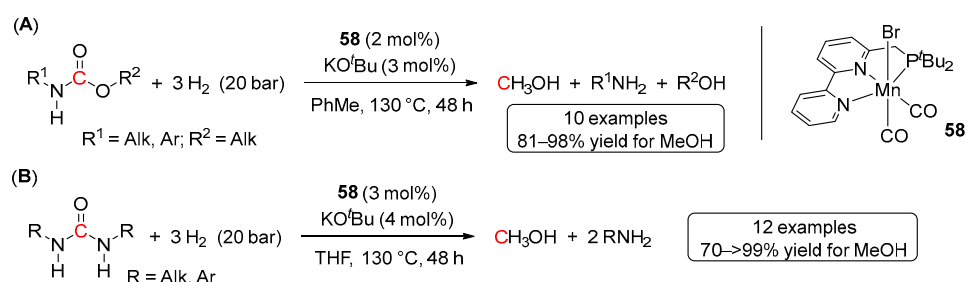
Scheme 40. CO₂ capture and hydrogenation to MeOH using valinol and pre-catalyst **4**.

Concerning other 2nd/3rd-row transition metals, hydrogenation of urea derivatives has been recently demonstrated by Kumar et al. using an iridium pre-catalyst **56** [99]. The reactions were conducted in THF at 130 °C and 50 bar of H₂ and showed excellent conversions (90–99%) of a series of disubstituted linear alkyl and aryl urea derivatives to MeOH and the corresponding amines (Scheme 41A). Remarkably, the system also proved effective in the hydrogenative depolymerization of poly-ureas reaching up to 62% conversions after 72 h at 140 °C and 50 bar of H₂, demonstrating the first example of hydrogenative recycling of poly-ureas (Scheme 41B). In contrast, cyclic urea derivatives were found to be incompatible with the reaction conditions, and no conversions of *N,N'*-trimethylene-urea and 1,3-dimethyl-2-imidazolidinone were detected. Noteworthy, several Ru pre-catalysts (such as complexes **47** (Scheme 35), **54** (Scheme 38C), and *trans*-RuCl₂(Ph₂PCH₂CH₂NH₂)₂ (**57**)) have been also tested in the hydrogenation of 1,3-diphenylurea and poly-ureas, but lower MeOH yields compared to iridium derivative **56** were observed [99].



Scheme 41. **56**-catalyzed hydrogenation of urea derivatives (A) and hydrogenative depolymerization of poly-ureas (B).

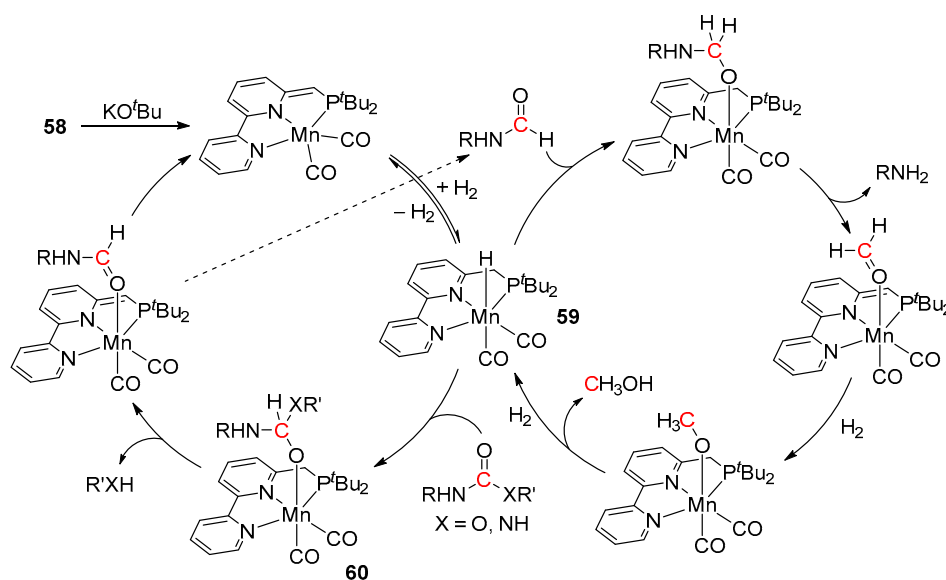
The first example of earth-abundant metal-catalyzed hydrogenation of both carbamates and urea derivatives was disclosed by Milstein and co-workers in 2019 [100]. Thus, using 2 mol% of manganese(I) PNN pre-catalyst **58** in the presence of 3 mol% of KO^tBu, a series of *N*-monosubstituted carbamates with aliphatic and aromatic substituents were hydrogenated to the corresponding amines, alcohols and MeOH (Scheme 42A). The reaction conditions (130 °C for 48 h, 20 bar of H₂) were comparable to those for analogous Ru systems (*vide infra*) resulting in good to excellent yields of MeOH (81–98%), although *N,N*-disubstituted substrates failed to produce any detectable amounts of MeOH, presumably due to steric reasons.



Scheme 42. **58**-catalyzed hydrogenation of carbamates (A) and urea derivatives (B).

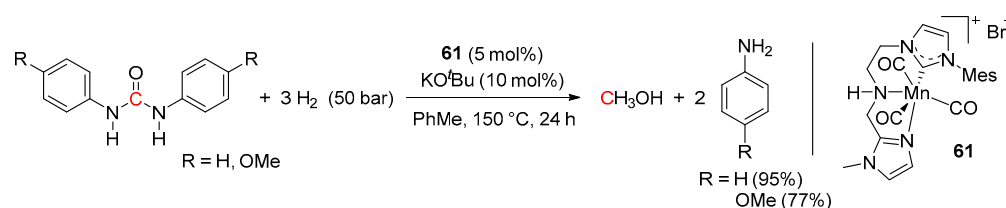
Similarly to carbamates, complex **58** proved highly active in the hydrogenation of disubstituted linear urea derivatives (Scheme 42B) [100]. In contrast to Ru complex **2**, which showed moderate conversions of tetra-substituted ureas (Scheme 37B), **58** turned out to be completely inactive in the hydrogenation of such substrates (even under 60 bar of H₂). On the other hand, slightly decreasing the steric hindrance of the substrate and switching to the trisubstituted 1-benzyl-3-(4-fluorobenzyl)-1-methylurea afforded 71% of MeOH.

The proposed MLC mechanism of **58**-catalyzed hydrogenation of carbamates and ureas is depicted in Scheme 43. The reactions are initiated by the treatment of complex **58** with KO^tBu under a hydrogen atmosphere, which generates a hydride species **59**, suggested as an active catalyst. The following migratory insertion of the substrate into the Mn-H bond of **59** affords the intermediate **60**, which then undergoes the C-N/O bond cleavage and elimination of the corresponding amine/alcohol by metal–ligand cooperation. This is followed by the regeneration of the catalyst **59** via heterolytic H₂ splitting accompanied by the release of *N*-formamide. The latter species is then converted via MLC to formaldehyde and then to MeOH, analogously to Ru systems discussed previously (see Section 3).



Scheme 43. The proposed mechanism of **58**-catalyzed hydrogenation of carbamates and ureas.

A more recent example of Mn-catalyzed hydrogenation of urea derivatives has been demonstrated by Wang and Liu using an NHC-based NNC-pincer pre-catalyst **61** (Scheme 44) [101]. Compared to complex **58**, the reactions required rather harsh conditions (150 °C, 50 bar of H₂) and resulted in 77–95% yields of the corresponding amines, whereas the yield of MeOH was not determined. Notably, the same system proved active in the hydrogenation of dibenzyl and diphenyl carbonates to the corresponding alcohols (83–90%) and in hydrogenative depolymerization of polycarbonates (polyethylene glycol terephthalate, bisphenol A polycarbonate and polycaprolactone) to give 89–96% yields of the corresponding monomers.



Scheme 44. **61**-catalyzed hydrogenation of urea derivatives.

6. Conclusions

Within the last decade, significant progress has been made in homogeneous transition metal-catalyzed hydrogenation of formates, formamides, carbonates, carbamates, and urea derivatives. The developments in this field have been mainly driven by the search for alternative routes to methanol from carbon dioxide, allowing for sustainable recycling of CO₂ into a green fuel and value-added chemicals. Compared to direct hydrogenation reactions, a combination of effective capture of CO₂ in the form of its organic derivatives with their further catalytic hydrogenation to MeOH offers energetically favorable pathways for chemical utilization of CO₂ without the need for energetically expensive desorption and compression processes, considered as major stumbling blocks to practical CO₂ capture and utilization technologies. Indeed, the practical viability of indirect hydrogenative conversion of CO₂ to MeOH via formates, formamides, and carbonates has been already demonstrated by several research groups, showing excellent CO₂-to-MeOH turnovers and operating under rather mild temperatures (as low as ≤100 °C) and H₂ pressures (mostly in 10–60 bar range). Remarkably, some of these systems proved effective in capturing and hydrogenating CO₂ from synthetic flue gas and even from air under atmospheric CO₂ pressure. Several research groups have also reported on effective catalyst recycling approaches, demonstrating another step forward toward applicable catalytic CO₂-to-MeOH technologies.

A comparison of catalytic activities of transition metal-based homogeneous systems in hydrogenation of CO₂ derivatives is shown in Table 1. Not surprisingly, in contrast to formates, formamides, and carbonates, which showed comparatively high turnovers in hydrogenation to MeOH (TON_{max} up to 9500; Table 1, entry 12), catalytic hydrogenation of carbamates and urea derivatives is developed to a lesser extent. The major obstacles here are associated with the significantly reduced electrophilicity of carbamates and ureas compared to other CO₂ derivatives. This resulted in generally higher catalyst loadings and prolonged reaction times under elevated temperatures, as well as rather low turnovers to MeOH (TON_{max} up to 97; Table 1, entry 43). Nonetheless, as proof of principle, a cascade conversion of CO₂ to MeOH via oxazolidinone derivatives has been recently disclosed (see Scheme 40).

Table 1. Comparison of catalytic activities of homogeneous catalysts based on different transition metals in the hydrogenation of CO₂ derivatives (the most active catalytic systems are highlighted in red) ^a.

Entry	Substrate	Catalyst	T, °C/t, h/P(H ₂), bar ^b	TON _{max} for MeOH	By-Products ^c	Ref.
<i>Formates</i>						
1		1 (Ru)	110/48/10	1155	- ^d	[34]
2		2 (Ru)	110/14/50	4700	- ^d	[34]
3		3 (Ru)	110/48/10	1215	- ^d	[34]
4		4 (Ru)	110/48/10	1365	- ^d	[34]
5		11 (Ir)	155/16/~83	- ^d	HCOOMe ^e	[37]
6		13 (Ru)	140/24/30	77	- ^d	[38]
7		15 (Co)	100/24/70	12	- ^d	[41]
8		16 (Mn)	110/30/30	43	- ^d	[42]
9		20 (Mn)	120/45/50	- ^d	HCOOMe ^e	[43]
<i>Formamides</i>						
10		23 (Ru)	155/18/50	99	- ^d	[48]
11		28 (Ru)	160/1/~51	4700	- ^d	[51]
12		30 (Ru)	170/30/~41	9500	- ^d	[55]
13		32 (Mn)	150/24/70	128	- ^d	[58]
14		34 (Fe)	120/16/62	4950	- ^d	[23]
15		36 (Ru)	110/32/~10	97	- ^d	[62]

Table 1. Cont.

Entry	Substrate	Catalyst	T, °C/t, h/P(H ₂), bar ^b	TON _{max} for MeOH	By-Products ^c	Ref.
16		37 (Fe)	110/3/20	300	- ^d	[63]
17		38 (Ru)	60/3/80	71	- ^d	[64]
18		39 (Mn)	100/16/30	50	- ^d	[66]
19		40 (Mo)	100/24/30	20	- ^d	[67]
20		41 (Ir)	110/16/40	21	- ^d	[68]
21		57 (Ru)	180/20/30	210	- ^d	[54]
<i>Acyclic carbonates</i>						
22		1 (Ru)	145/1/~61 145/3.5/~41	2500 2500	- ^d - ^d	[34] [34]
23		2 (Ru)	110/14/~51	4400	- ^d	[34]
24		13 (Ru)	140/16/50	94 (6219 in neat Me₂CO₃)	- ^d	[73]
25		16 (Mn)	110/30/30	50	- ^d	[42]
26		31 (Ru)	140/24/200	3333	- ^d	[57]
27		43 (Ru)	140/24/~51	200	- ^d	[75]
28		44 (Ru)	135/24/~51	99	- ^d	[78]
29		45 (Co)	120/18/50	50	- ^d	[79]
30		46 (Co)	160/20/60	75	- ^d	[80]
<i>Cyclic carbonates</i>						
31		16 (Mn)	110/50/50	50	- ^d	[42]
32		32 (Mn)	120/26/30	50	- ^d	[84]
33		43 (Ru)	140/24/~51	196	- ^d	[75]
34		44 (Ru)	130/20/~51	98	- ^d	[78]
35		45 (Co)	120/18/50	50	- ^d	[79]
36		46 (Co)	160/20/60	92	- ^d	[80]
37		47 (Ru)	140/4/~51	4950	- ^d	[81]
38		RuHCl(CO)(PPh ₃) ₃ / 48	130/12/50	44	- ^d	[82]
<i>Carbonate salts</i>						
39	ammonium carbonate	23 (Ru)	140/72/70	184	- ^d	[90]
40	potassium carbonate	23 (Ru)	140/20/70	200	- ^d	[91]
41	potassium bicarbonate	23 (Ru)	140/48/70	184	- ^d	[91]
42	potassium formate	23 (Ru)	140/48/70	200	- ^d	[91]
<i>Carbamates</i>						
43		2 (Ru)	110/48/~10	97	- ^d	[34]
44		4 (Ru)	135/72/60	~24	- ^d	[98]
45		58 (Mn)	130/24/50	49	- ^d	[100]
<i>Urea derivatives</i>						
46		2 (Ru)	110/72/~14	47	- ^d	[96]
47		4 (Ru)	170/96/60	87	- ^d	[97]
48		13 (Ru)	140/24/50	- ^d	Methylamines (32%) ^f	[73]
49		54 (Ru)	170/168/60	79	- ^d	[97]
50		55 (Ru)	170/168/60	81	- ^d	[97]
51		56 (Ir)	130/24/50	47	- ^d	[99]
52		58 (Mn)	130/48/20	33	- ^d	[100]
53		61 (Mn)	150/24/50	19	- ^d	[101]

^a Only monomeric substrates are considered. No cascade/tandem approaches for CO₂ hydrogenation in the presence of alcohols/amines are listed herein. The most active systems (in terms of TON) are highlighted in red.

^b Conditions for the best TON are shown. ^c Only CO₂-derived by-products are shown. ^d No by-products reported.

^e The reactions were tested with ethyl formate, showing the formation of a mixture of MeOH, EtOH, and methyl formate. Only the overall yield of MeOH and HCOOMe was reported. ^f Hydrogenation of 1,3-diphenylurea was tested and resulted in 66% of aniline, 24% of methyl aniline, 8% of dimethylaniline.

Overall, despite these exciting achievements, the majority of the developed catalytic systems for the reduction of CO₂ derivatives are based on ruthenium (18 Ru complexes out of total of 34 complexes; Table 1), which showed the highest turnovers to MeOH for all substrates. Considering the low natural abundance of ruthenium, a shift towards more economical catalysts is highly desirable. Several catalytic systems based on abundant 3d metals (Mn, Fe, Co) have been recently disclosed, but these examples are still scarce and generally show lower activities compared to Ru catalysts (Table 1). Besides, further improvements in the thermal stability of catalytic systems and their robustness towards poisoning (for instance by CO) would significantly improve their practical attractiveness. Nevertheless, the obtained exciting results drive the research in catalytic reduction of CO₂ and CO₂ derivatives forward, and it is expected that the intensity of research in this direction will only increase in the coming years.

Author Contributions: Conceptualization, A.Y.K.; writing—original draft preparation, T.A., A.A. and A.Y.K.; writing—review and editing, T.A., A.A. and A.Y.K.; supervision, A.Y.K.; funding acquisition, A.Y.K. All authors have read and agreed to the published version of the manuscript.

Funding: This work was supported by Nazarbayev University through the collaborative research program (CRP) (grant No. 021220CRP2122).

Conflicts of Interest: The authors declare no conflict of interest. The funders had no role in the design of the study; in the collection, analyses, or interpretation of data; in the writing of the manuscript; or in the decision to publish the results.

References

1. Liu, G. (Ed.) *Greenhouse Gases—Capturing, Utilization and Reduction*; InTech: Rijeka, Croatia, 2012.
2. Global Monitoring Laboratory. Trends in Atmospheric Carbon Dioxide. Available online: <https://gml.noaa.gov/ccgg/trends/> (accessed on 14 June 2023).
3. *Key Renewables Trends*; International Energy Agency: Paris, France, 2015.
4. Shen, M.; Kong, F.; Tong, L.; Luo, Y.; Yin, S.; Liu, C.; Zhang, P.; Wang, L.; Chu, P.K.; Ding, Y. Carbon capture and storage (CCS): Development path based on carbon neutrality and economic policy. *Carb. Neutrality* **2022**, *1*, 37. [[CrossRef](#)]
5. Dods, M.N.; Kim, E.L.; Long, J.R.; Weston, S.C. Deep CCS: Moving beyond 90% Carbon Dioxide Capture. *Environ. Sci. Technol.* **2021**, *55*, 8524–8534. [[CrossRef](#)]
6. Osman, A.I.; Hefny, M.; Maksoud, M.I.A.A.; Elgarahy, A.M.; Rooney, D.W. Recent advances in carbon capture storage and utilization technologies: A review. *Environ. Chem. Lett.* **2021**, *19*, 797–849. [[CrossRef](#)]
7. Gao, W.; Liang, S.; Wang, R.; Jiang, Q.; Zhang, Y.; Zheng, Q.; Xie, B.; Toe, C.Y.; Zhu, X.; Wang, J.; et al. Industrial carbon dioxide capture and utilization: State of the art and future challenges. *Chem. Soc. Rev.* **2020**, *49*, 8584–8686. [[CrossRef](#)] [[PubMed](#)]
8. Knez, Ž.; Markočič, E.; Leitgeb, M.; Primožič, M.; Knez Hrnčič, M.; Škerget, M. Industrial applications of supercritical fluids: A review. *Energy* **2014**, *77*, 235–243. [[CrossRef](#)]
9. Prasad, S.K.; Sangwai, J.S.; Byun, H.-S. A review of the supercritical CO₂ fluid applications for improved oil and gas production and associated carbon storage. *J. CO₂ Util.* **2023**, *72*, 102479. [[CrossRef](#)]
10. Tan, Y.; Li, Q.; Xu, L.; Ghaffar, A.; Zhou, X.; Li, P. A critical review of carbon dioxide enhanced oil recovery in carbonate reservoirs. *Fuel* **2022**, *328*, 125256. [[CrossRef](#)]
11. Ali, M.; Jha, N.K.; Pal, N.; Keshavarz, A.; Hoteit, H.; Sarmadivaleh, M. Recent advances in carbon dioxide geological storage, experimental procedures, influencing parameters, and future outlook. *Earth Sci. Rev.* **2022**, *225*, 103895. [[CrossRef](#)]
12. Sahoo, P.K.; Zhang, Y.; Das, S. CO₂-Promoted Reactions: An Emerging Concept for the Synthesis of Fine Chemicals and Pharmaceuticals. *ACS Catal.* **2021**, *11*, 3414–3442. [[CrossRef](#)]
13. Zhang, Y.; Zhang, T.; Das, S. Catalytic transformation of CO₂ into C1 chemicals using hydrosilanes as a reducing agent. *Green Chem.* **2020**, *22*, 1800–1820. [[CrossRef](#)]
14. Bai, S.-T.; De Smet, G.; Liao, Y.; Sun, R.; Zhou, C.; Beller, M.; Maes, B.U.W.; Sels, B.F. Homogeneous and heterogeneous catalysts for hydrogenation of CO₂ to methanol under mild conditions. *Chem. Soc. Rev.* **2021**, *50*, 4259–4298. [[CrossRef](#)]
15. Sun, R.; Liao, Y.; Bai, S.-T.; Zheng, M.; Zhou, C.; Zhang, T.; Sels, B.F. Heterogeneous catalysts for CO₂ hydrogenation to formic acid/formate: From nanoscale to single atom. *Energy Environ. Sci.* **2021**, *14*, 1247–1285. [[CrossRef](#)]
16. Dixneuf, P.H. A bridge from CO₂ to methanol. *Nat. Chem.* **2011**, *3*, 578–579. [[CrossRef](#)] [[PubMed](#)]
17. Federsel, C.; Jackstell, R.; Beller, M. State-of-the-Art Catalysts for Hydrogenation of Carbon Dioxide. *Angew. Chem. Int. Ed.* **2010**, *49*, 6254–6257. [[CrossRef](#)]
18. Sakakura, T.; Choi, J.-C.; Yasuda, H. Transformation of Carbon Dioxide. *Chem. Rev.* **2007**, *107*, 2365–2387. [[CrossRef](#)]
19. ChemAnalyst. Decode the Future of Methanol. Available online: <https://www.chemanalyst.com/industry-report/methanol-market-219> (accessed on 14 June 2023).

20. Palo, D.R.; Dagle, R.A.; Holladay, J.D. Methanol Steam Reforming for Hydrogen Production. *Chem. Rev.* **2007**, *107*, 3992–4021. [CrossRef]
21. Sordakis, K.; Tang, C.; Vogt, L.K.; Junge, H.; Dyson, P.J.; Beller, M.; Laurenczy, G. Homogeneous Catalysis for Sustainable Hydrogen Storage in Formic Acid and Alcohols. *Chem. Rev.* **2018**, *118*, 372–433. [CrossRef] [PubMed]
22. For example: Sklyaruk, J.; Zubar, V.; Borghs, J.C.; Rueping, M. Methanol as the Hydrogen Source in the Selective Transfer Hydrogenation of Alkynes Enabled by a Manganese Pincer Complex. *Org. Lett.* **2020**, *22*, 6067–6071. [CrossRef]
23. Lane, E.M.; Zhang, Y.; Hazari, N.; Bernskoetter, W.H. Sequential Hydrogenation of CO₂ to Methanol Using a Pincer Iron Catalyst. *Organometallics* **2019**, *38*, 3084–3091. [CrossRef]
24. Li, Y.-N.; Ma, R.; He, L.-N.; Diao, Z.-F. Homogeneous hydrogenation of carbon dioxide to methanol. *Catal. Sci. Technol.* **2014**, *4*, 1498–1512. [CrossRef]
25. Sen, R.; Goepfert, A.; Prakash, G.K.S. Homogeneous Hydrogenation of CO₂ and CO to Methanol: The Renaissance of Low-Temperature Catalysis in the Context of the Methanol Economy. *Angew. Chem. Int. Ed.* **2022**, *61*, e202207278. [CrossRef] [PubMed]
26. Artz, J.; Müller, T.E.; Thenert, K.; Kleinekorte, J.; Meys, R.; Sternberg, A.; Bardow, A.; Leitner, W. Sustainable Conversion of Carbon Dioxide: An Integrated Review of Catalysis and Life Cycle Assessment. *Chem. Rev.* **2018**, *118*, 434–504. [CrossRef] [PubMed]
27. Buysch, H.J. *Ullmann's Encyclopedia of Industrial Chemistry*; Wiley-VCH: Weinheim, Germany, 2012; Volume 7, pp. 45–71.
28. Schäffner, B.; Schäffner, F.; Verevkin, S.P.; Börner, A. Organic Carbonates as Solvents in Synthesis and Catalysis. *Chem. Rev.* **2010**, *110*, 4554–4581. [CrossRef]
29. Dabral, S.; Schaub, T. The Use of Carbon Dioxide (CO₂) as a Building Block in Organic Synthesis from an Industrial Perspective. *Adv. Synth. Catal.* **2019**, *361*, 223–246. [CrossRef]
30. ChemAnalyst. Decode the Future of Urea. Available online: <https://www.chemanalyst.com/industry-report/urea-market-666> (accessed on 14 June 2023).
31. Kumar, A.; Bhardwaj, R.; Mandal, S.K.; Choudhury, J. Transfer Hydrogenation of CO₂ and CO₂ Derivatives using Alcohols as Hydride Sources: Boosting and H₂-Free Alternative Strategy. *ACS Catal.* **2022**, *12*, 8886–8903. [CrossRef]
32. Gormley, R.J.; Rao, V.U.S.; Soong, Y. Methyl formate hydrogenolysis for low-temperature methanol synthesis. *Appl. Catal. A* **1992**, *87*, 81–101. [CrossRef]
33. Iwasa, N.; Terashita, M.; Arai, M.; Takezawa, N. New catalytic functions of Pd and Pt catalysts for hydrogenolysis of methyl formate. *React. Kinet. Catal. Lett.* **2001**, *74*, 93–98. [CrossRef]
34. Balaraman, E.; Gunanathan, C.; Zhang, J.; Shimon, L.J.W.; Milstein, D. Efficient hydrogenation of organic carbonates, carbamates and formates indicates alternative routes to methanol based on CO₂ and CO. *Nat. Chem.* **2011**, *3*, 609–614. [CrossRef]
35. Li, H.; Wen, M.; Wang, Z.-X. Computational Mechanistic Study of the Hydrogenation of Carbonate to Methanol Catalyzed by the Ru^{II}PNN Complex. *Inorg. Chem.* **2012**, *51*, 5716–5727. [CrossRef]
36. Huff, C.A.; Sanford, M.S. Cascade Catalysis for the Homogeneous Hydrogenation of CO₂ to Methanol. *J. Am. Chem. Soc.* **2011**, *133*, 18122–18125. [CrossRef]
37. Chu, W.-Y.; Culakova, Z.; Wang, B.T.; Goldberg, K.I. Acid-Assisted Hydrogenation of CO₂ to Methanol in a Homogeneous Catalytic Cascade System. *ACS Catal.* **2019**, *9*, 9317–9326. [CrossRef]
38. Wesselbaum, S.; vom Stein, T.; Klankermayer, J.; Leitner, W. Hydrogenation of Carbon Dioxide to Methanol by Using a Homogeneous Ruthenium-Phosphine Catalyst. *Angew. Chem. Int. Ed.* **2012**, *51*, 7499–7502. [CrossRef]
39. Leitner, W. Carbon Dioxide as a Raw Material: The Synthesis of Formic Acid and Its Derivatives from CO₂. *Angew. Chem. Int. Ed.* **1995**, *34*, 2207–2221. [CrossRef]
40. Jessop, P.G.; Ikariya, T.; Noyori, R. Homogeneous Hydrogenation of Carbon Dioxide. *Chem. Rev.* **1995**, *95*, 259–272. [CrossRef]
41. Schneidewind, J.; Adam, R.; Baumann, W.; Jackstell, R.; Beller, M. Low-Temperature Hydrogenation of Carbon Dioxide to Methanol with a Homogeneous Cobalt Catalyst. *Angew. Chem. Int. Ed.* **2017**, *56*, 1890–1893. [CrossRef]
42. Kumar, A.; Janes, T.; Espinosa-Jalapa, N.A.; Milstein, D. Manganese Catalyzed Hydrogenation of Organic Carbonates to Methanol and Alcohols. *Angew. Chem. Int. Ed.* **2018**, *57*, 12076–12080. [CrossRef] [PubMed]
43. Kuß, D.A.; Hölscher, M.; Leitner, M. Hydrogenation of CO₂ to Methanol with Mn-PNP-Pincer Complexes in the Presence of Lewis Acids: The Formate Resting State Unleashed. *ChemCatChem* **2021**, *13*, 3319–3323.
44. Kuß, D.A.; Hölscher, M.; Leitner, W. Combined Computational and Experimental Investigation on the Mechanism of CO₂ Hydrogenation to Methanol with Mn-PNP-Pincer Catalysts. *ACS Catal.* **2022**, *12*, 15310–15322.
45. Khalimon, A.Y.; Gudun, K.A.; Hayrapetyan, D. Base Metal Catalysts for Deoxygenative Reduction of Amides to Amines. *Catalysts* **2019**, *9*, 490. [CrossRef]
46. Khalimon, A.Y. Deoxygenative Hydroboration of Carboxamides: A Versatile and Selective Synthetic Approach to Amines. *Dalton Trans.* **2021**, *50*, 17455–17466. [CrossRef]
47. Werkmeister, S.; Junge, K.; Beller, M. Catalytic Hydrogenation of Carboxylic Acid Esters, Amides, and Nitriles with Homogeneous Catalysts. *Org. Process Res. Dev.* **2014**, *18*, 289–302. [CrossRef]
48. Rezayee, N.M.; Huff, C.A.; Sanford, M.S. Tandem Amine and Ruthenium-Catalyzed Hydrogenation of CO₂ to Methanol. *J. Am. Chem. Soc.* **2015**, *137*, 1028–1031. [CrossRef] [PubMed]
49. Kar, S.; Sen, R.; Kothandaraman, J.; Goepfert, A.; Chowdhury, R.; Munoz, S.B.; Haiges, R.; Prakash, G.K.S. Mechanistic Insights into Ruthenium-Pincer-Catalyzed Amine-Assisted Homogeneous Hydrogenation of CO₂ to Methanol. *J. Am. Chem. Soc.* **2019**, *141*, 3160–3170. [CrossRef]

50. Mandal, S.C.; Rawat, K.S.; Nandi, S.; Pathak, B. Theoretical insights into CO₂ hydrogenation to methanol by a Mn-PNP complex. *Catal. Sci. Technol.* **2019**, *9*, 1867–1878. [[CrossRef](#)]
51. Zhang, L.; Han, Z.; Zhao, X.; Wang, Z.; Ding, K. Highly Efficient Ruthenium-Catalyzed N-Formylation of Amines with H₂ and CO₂. *Angew. Chem. Int. Ed.* **2015**, *54*, 6186–6189. [[CrossRef](#)]
52. Kothandaraman, J.; Goepfert, A.; Czaun, M.; Olah, G.A.; Prakash, G.K.S. Conversion of CO₂ from Air into Methanol Using a Polyamine and a Homogeneous Ruthenium Catalyst. *J. Am. Chem. Soc.* **2016**, *138*, 778–781. [[CrossRef](#)] [[PubMed](#)]
53. Kar, S.; Sen, R.; Goepfert, A.; Prakash, G.K.S. Integrative CO₂ Capture and Hydrogenation to Methanol with Reusable Catalyst and Amine: Toward a Carbon Neutral Methanol Economy. *J. Am. Chem. Soc.* **2018**, *140*, 1580–1583. [[CrossRef](#)]
54. Everett, M.; Wass, D.F. Highly productive CO₂ hydrogenation to methanol—A tandem catalytic approach via amide intermediates. *Chem. Commun.* **2017**, *53*, 9502–9504. [[CrossRef](#)]
55. Zhang, F.-H.; Liu, C.; Li, W.; Tian, G.-L.; Xie, J.-H.; Zhou, Q.-L. An Efficient Ruthenium Catalyst Bearing Tetradentate Ligand for Hydrogenations of Carbon Dioxide. *Chin. J. Chem.* **2018**, *36*, 1000–1002. [[CrossRef](#)]
56. Yoshimura, A.; Watari, R.; Kuwata, S.; Kayaki, Y. Poly(ethyleneimine)-Mediated Consecutive Hydrogenation of Carbon Dioxide to Methanol with Ru Catalysts. *Eur. J. Inorg. Chem.* **2019**, *2019*, 2375–2380. [[CrossRef](#)]
57. Diehl, T.; Lanzerath, P.; Franciò, G.; Leitner, W. A Self-Separating Multiphasic System for Catalytic Hydrogenation of CO₂ and CO₂-Derivatives to Methanol. *ChemSusChem* **2022**, *15*, e202201250. [[CrossRef](#)] [[PubMed](#)]
58. Kar, S.; Goepfert, A.; Kothandaraman, J.; Prakash, G.K.S. Manganese-Catalyzed Sequential Hydrogenation of CO₂ to Methanol via Formamide. *ACS Catal.* **2017**, *7*, 6347–6351. [[CrossRef](#)]
59. Ribeiro, A.P.C.; Martins, L.M.D.R.S.; Pombeiro, A.J.L. Carbon dioxide-to-methanol single-pot conversion using a C-scorpionate iron(II) catalyst. *Green Chem.* **2017**, *19*, 4811–4815. [[CrossRef](#)]
60. Bernskoetter, W.H.; Hazari, N. Reversible Hydrogenation of Carbon Dioxide to Formic Acid and Methanol: Lewis Acid Enhancement of Base Metal Catalysts. *Acc. Chem. Res.* **2017**, *50*, 1049–1058. [[CrossRef](#)]
61. Wei, D.; Shi, X.; Junge, H.; Du, C.; Beller, M. Carbon neutral hydrogen storage and release cycles based on dual-functional roles of formamides. *Nat. Commun.* **2023**, *14*, 3726. [[CrossRef](#)]
62. Balaraman, E.; Gnanaprakasam, B.; Shimon, L.J.W.; Milstein, D. Direct Hydrogenation of Amides to Alcohols and Amines under Mild Conditions. *J. Am. Chem. Soc.* **2010**, *132*, 16756–16758. [[CrossRef](#)]
63. Rezayee, N.M.; Samblanet, D.C.; Sanford, M.S. Iron-Catalyzed Hydrogenation of Amides to Alcohols and Amines. *ACS Catal.* **2016**, *6*, 6377–6383. [[CrossRef](#)]
64. Miura, T.; Naruto, V.; Toda, K.; Shimomura, T.; Saito, S. Multifaceted catalytic hydrogenation of amides via diverse activation of a sterically confined bipyridine-ruthenium framework. *Sci. Rep.* **2017**, *7*, 1586. [[CrossRef](#)]
65. Jayrathne, U.; Zhang, Y.; Hazari, N.; Bernskoetter, W.H. Selective Iron-Catalyzed Deaminative Hydrogenation of Amides. *Organometallics* **2017**, *36*, 409–416. [[CrossRef](#)]
66. Papa, V.; Cabrero-Antonino, J.R.; Alberico, E.; Spanneberg, A.; Junge, K.; Junge, H.; Beller, M. Efficient and selective hydrogenation of amides to alcohols and amines using a well-defined manganese-PNN pincer complex. *Chem. Sci.* **2017**, *8*, 3576–3585. [[CrossRef](#)]
67. Leischner, T.; Suarez, L.A.; Spennenberg, A.; Junge, K.; Nova, A.; Beller, M. Highly selective hydrogenation of amides catalysed by a molybdenum pincer complex: Scope and mechanism. *Chem. Sci.* **2019**, *10*, 10566–10576. [[CrossRef](#)] [[PubMed](#)]
68. Ravn, A.K.; Rezayee, N.M. The Investigation of a Switchable Iridium Catalyst for the Hydrogenation of Amides: A Case Study of C–O Versus C–N Bond Scission. *ACS Catal.* **2022**, *12*, 11927–11933. [[CrossRef](#)]
69. Dibenedetto, A.; Angelini, A. Synthesis of Organic Carbonates. In *Advances in Inorganic Chemistry*; Aresta, M., van Eldik, R., Eds.; Academic Press: Cambridge, MA, USA, 2014; Volume 66, pp. 25–81.
70. Parker, H.L.; Sherwood, J.; Hunt, A.J.; Clark, J.H. Cyclic Carbonates as Green Alternative Solvents for the Heck Reaction. *ACS Sustain. Chem. Eng.* **2014**, *2*, 1739–1742.
71. Ma, J.; Sun, N.; Zhang, X.; Zhao, N.; Xiao, F.; Wei, W.; Sun, Y. A short review of catalysis for CO₂ conversion. *Catal. Today* **2009**, *148*, 221–231. [[CrossRef](#)]
72. Cokoja, M.; Bruckmeier, C.; Rieger, B.; Herrmann, W.A.; Kühn, F.E. Transformation of Carbon Dioxide with Homogeneous Transition-Metal Catalysts: A Molecular Solution to a Global Challenge? *Angew. Chem. Int. Ed.* **2011**, *50*, 8510–8537. [[CrossRef](#)] [[PubMed](#)]
73. vom Stein, T.; Meuresch, M.; Limper, D.; Schmitz, M.; Hölscher, M.; Coetzee, J.; Cole-Hamilton, D.L.; Klammkermayer, J.; Leitner, W. Highly Versatile Catalytic Hydrogenation of Carboxylic and carbonic Acid Derivatives using a Ru-Triphos Complex: Molecular Control over Selectivity and Substrate Scope. *J. Am. Chem. Soc.* **2014**, *136*, 13217–13225. [[CrossRef](#)]
74. Geilen, F.M.A.; Engendahl, B.; Hölscher, M.; Klammkermayer, J.; Leitner, W. Selective Homogeneous Hydrogenation of Biogenic carboxylic Acids with [Ru(TriPhos)H]⁺: A Mechanistic Study. *J. Am. Chem. Soc.* **2011**, *133*, 14349–14358. [[CrossRef](#)]
75. Chen, J.; Zhu, H.; Chen, J.; Le, Z.-G.; Tu, T. Synthesis, Characterization and Catalytic Application of Pyridine-bridged N-Heterocyclic carbene-Ruthenium Complexes in the Hydrogenation of Carbonates. *Chem. Asian J.* **2017**, *12*, 2809–2812. [[CrossRef](#)]
76. Alberti, C.; Eckelt, S.; Enthaler, S. Ruthenium-Catalyzed Hydrogenative Depolymerization of End-of-Life Poly(bisphenol A carbonate). *ChemistrySelect* **2019**, *4*, 12268–12271. [[CrossRef](#)]
77. Kindler, T.-O.; Alberti, C.; Sundermeier, J.; Enthaler, S. Hydrogenative Depolymerization of End-of-Life Poly(Bisphenol A Carbonate) catalyzed by a Ruthenium MACHO-Complex. *ChemistryOpen* **2019**, *8*, 1410–1412. [[CrossRef](#)]

78. Mujahed, S.; Richter, M.S.; Kirillov, E.; Hey-Hawkins, E.; Gelman, D. A High-valent Ru-PCP Pincer Catalyst for the Hydrogenation of Organic Carbonates. *Isr. J. Chem.* **2023**, e202300037. [[CrossRef](#)]
79. Ferretti, F.; Scharnagl, F.K.; Dall'Anese, A.; Jackstell, R.; Dastgir, S.; Beller, M. Additive-free cobalt-catalyzed hydrogenation of carbonates to methanol and alcohols. *Catal. Sci. Technol.* **2019**, *9*, 3548–3553. [[CrossRef](#)]
80. Dahiya, P.; Gangwar, M.K.; Sundararaju, B. Well-defined Cp*Co(III)-catalyzed Hydrogenation of Carbonates and Polycarbonates. *ChemCatChem* **2021**, *13*, 934–939. [[CrossRef](#)]
81. Han, Z.; Rong, L.; Wu, J.; Zhang, L.; Wang, Z.; Ding, K. Catalytic Hydrogenation of Cyclic Carbonates: A Practical Approach from CO₂ and Epoxides to Methanol and Diols. *Angew. Chem. Int. Ed.* **2012**, *51*, 13041–13045. [[CrossRef](#)]
82. Wu, X.; Ji, L.; Ji, Y.; Elageed, E.H.M.; Gao, G. Hydrogenation of ethylene carbonate catalyzed by lutidine-bridged N-heterocyclic carbene ligands and ruthenium precursors. *Catal. Commun.* **2016**, *85*, 57–60. [[CrossRef](#)]
83. Zubar, V.; Lebedev, Y.; Azofra, L.M.; Cavallo, L.; El-Sepegly, O.; Rueping, M. Hydrogenation of CO₂-Derived Carbonates and Polycarbonates to Methanol and Diols by Metal-Ligand Cooperative Manganese Catalysis. *Angew. Chem. Int. Ed.* **2018**, *57*, 13439–13443. [[CrossRef](#)] [[PubMed](#)]
84. Kaithal, A.; Hölscher, M.; Leitner, W. Catalytic Hydrogenation of Cyclic Carbonates using Manganese Complexes. *Angew. Chem. Int. Ed.* **2018**, *57*, 13449–13453. [[CrossRef](#)]
85. Kothandaraman, J.; Heldebrant, D.J. Catalytic coproduction of methanol and glycol in one pot from epoxide, CO₂, and H₂. *RSC Adv.* **2020**, *10*, 42557–42563. [[CrossRef](#)]
86. Kothandaraman, J.; Dagle, R.A.; Dagle, V.L.; Davidson, S.D.; Walter, E.D.; Burton, S.D.; Hoyt, D.W.; Heldebrant, D.J. Condensed-phase low temperature heterogeneous hydrogenation of CO₂ to methanol. *Catal. Sci. Technol.* **2018**, *8*, 5098–5103. [[CrossRef](#)]
87. Lao, D.B.; Galan, B.R.; Linehan, J.C.; Heldebrant, D.J. The steps of activating a prospective CO₂ hydrogenation catalyst with combined CO₂ capture and reduction. *Green Chem.* **2016**, *18*, 4871–4874. [[CrossRef](#)]
88. Kothandaraman, J.; Heldebrant, D.J. Towards environmentally benign capture and conversion: Heterogeneous metal catalyzed CO₂ hydrogenation in CO₂ capture solvents. *Green Chem.* **2020**, *22*, 828–834. [[CrossRef](#)]
89. Rainbolt, J.E.; Koech, P.K.; Yonker, C.R.; Zheng, F.; Main, D.; Weaver, M.L.; Linehan, J.C.; Helderant, D.J. Anhydrous tertiary alkanolamines as hybrid chemical and physical CO₂ capture reagents with pressure-swing regeneration. *Energy Environ. Sci.* **2011**, *4*, 480–484. [[CrossRef](#)]
90. Sen, R.; Koch, C.J.; Goeppert, A.; Prakash, G.K.S. Tertiary Amine-Ethylene Glycol Based Tandem CO₂ Capture and Hydrogenation to Methanol: Direct Utilization of Post-Combustion CO₂. *ChemSusChem* **2020**, *13*, 6318–6322.
91. Sen, R.; Goeppert, A.; Kar, S.; Prakash, G.K.S. Hydroxide Based Integrated CO₂ Capture from Air and Conversion to Methanol. *J. Am. Chem. Soc.* **2020**, *142*, 4544–4549. [[CrossRef](#)]
92. Pritchard, J.; Filonenko, G.A.; van Putten, R.; Hensen, E.J.M.; Pidko, E.A. Heterogeneous and homogeneous catalysts for the hydrogenation of carboxylic acid derivatives: History, advances and future directions. *Chem. Rev.* **2015**, *44*, 3808–3833.
93. Ohgomori, Y.; Mori, S.; Yoshida, S.-I.; Watanabe, Y. The Role of Amide Solvents in the Formation of ethylene Glycol from Synthesis Gas. *J. Mol. Catal.* **1987**, *40*, 223–228. [[CrossRef](#)]
94. Imperato, G.; Höger, S.; Lenoir, D.; König, B. Low melting sugar-urea-salt mixtures as solvents for organic reactions—Estimation of polarity and use in catalysis. *Green Chem.* **2006**, *8*, 1051–1055. [[CrossRef](#)]
95. Kocienski, P.J. *Protecting Groups*, 3rd ed.; Thieme: New York, NY, USA, 2005.
96. Balaraman, E.; Ben-David, Y.; Milstein, D. Unprecedented Catalytic Hydrogenation of Urea Derivatives to Amines and Methanol. *Angew. Chem. Int. Ed.* **2011**, *50*, 11702–11705. [[CrossRef](#)]
97. Xie, Y.; Hu, P.; Ben-David, Y.; Milstein, D. A Reversible Liquid Organic Carrier System Based on Methanol-Ethylenediamine and Ethylene Urea. *Angew. Chem. Int. Ed.* **2019**, *58*, 5105–5109. [[CrossRef](#)] [[PubMed](#)]
98. Khusnutdinova, J.R.; Garg, J.A.; Milstein, D. Combining Low-Pressure CO₂ Capture and Hydrogenation to Form Methanol. *ACS Catal.* **2015**, *5*, 2416–2422. [[CrossRef](#)]
99. Kumar, A.; Luk, J. Catalytic Hydrogenation of Urea Derivatives and Polyureas. *Eur. J. Org. Chem.* **2021**, *2021*, 4546–4550. [[CrossRef](#)]
100. Das, U.K.; Kumar, A.; Ben-David, Y.; Iron, M.A.; Milstein, D. Manganese Catalyzed Hydrogenation of Carbamates and Urea Derivatives. *J. Am. Chem. Soc.* **2019**, *141*, 12962–12966. [[CrossRef](#)] [[PubMed](#)]
101. Wei, Z.; Li, H.; Wang, Y.; Liu, Q. A Tailored Versatile and Efficient NHC-Based NNC-Pincer Manganese Catalyst for Hydrogenation of Polar Unsaturated Compounds. *Angew. Chem. Int. Ed.* **2023**, *62*, e202301042. [[CrossRef](#)] [[PubMed](#)]

Disclaimer/Publisher's Note: The statements, opinions and data contained in all publications are solely those of the individual author(s) and contributor(s) and not of MDPI and/or the editor(s). MDPI and/or the editor(s) disclaim responsibility for any injury to people or property resulting from any ideas, methods, instructions or products referred to in the content.